IN VIVO TRACKING OF MESENCHYMAL STEM CELL RECRUITMENT TO TISSUE SCAFFOLDS

by

MANWU SUN

Presented to the Faculty of the Graduate School of

The University of Texas at Arlington in Partial Fulfillment

of the Requirements

for the Degree of

MASTER OF SCIENCE IN BIOENGINEERING

THE UNIVERSITY OF TEXAS AT ARLINGTON

MAY 2010

ACKNOWLEDGEMENTS

I take this opportinity to acknowledge Dr Liping Tang, my mentor, for not just being a wounderful guide but for having given me an opportunity to work in his lab. It is the result of my countless interactions with him, that, today I believe I can someday create a niche for myself in science.

I would also like to thank Dr Yang and Dr Nguyen for having spare their valuable time to review my work and also providing valuable inputs and suggestions whenever I have sought their help.

I acknowledge the efforts of Yi-Ting Tsai for conducting the pilot studies. Working with Yi-Ting on this study was a very good experience. The time taken by Dr Shen in our lab, to train me to isolate bone marrow and culture is greatly appreciated. My heartfelt gratitude for the support of all my colleagues in the lab, especially Ashwin, Paul, and Cheng-Yu.

It goes without saying that I own everything to my family back in Taiwan which has been extremely supportive through every phase of my life. Acknowledging my family, in particular my parents is something that I cannot do on a piece of paper.

April 1, 2010

ABSTRACT

IN VIVO TRACKING OF MESENCHYMAL STEM CELL

RECRUITMENT TO TISSUE SCAFFOLDS

Manwu Sun, M.S

The University of Texas at Arlington, 2010

Supervising Professor: Liping Tang

The term "Stem cells" has been extensively used to describe precursor undifferentiated cells that have the capacity to self-renew and can also give rise to multiple tissue types. Many studies have been shown improved functional outcome after treated with stem cell therapy. However, almost all of these investigations were analyzed based on histological evaluations which are time-consuming, expensive and fail to provide 3 dimensional and real-time information about stem cell responses. Therefore, there is a need for the development of new method to investigate the migration of stem cells in vivo. Recent evidence supports that fluorescence imaging system offer both near-infrared resolution and whole-body imaging capability.

The purpose of this study was to examine whether using *in vivo* imaging method to track and to identify the localization *in vivo* of the transplanted stem cells to the site of injury after different routes (IP/ IV) of injection at different time points. Taking advantage of recent progress of whole-body imaging system, bone marrow derived mesenchymal stem cells were labeled with

near-infrared imaging agents. Following transplantation, the migration of mesenchymal stem cells was monitored in real-time.

To study whether the localized release of chemokines affect stem cell recruitment, scaffolds capable of releasing stromal cell derived-1 alpha (SDF-1α) or Erythropoietin (EPO) were fabricated. Our results have supported our hypothesis that the release of both chemokines enhances stem cell recruitment using whole-body imaging system. Such observations are also confirmed by histological results. The results of this work have lead to the establishment of an imaging system which allows real-time stem cell responses to tissue scaffold implants in animals.

TABLE OF CONTENTS

LIST OF FIGURES

CHAPTER 1

INTRODUCTION

Stem-cell-based therapies are an attractive option for the treatment of tissue repair and regeneration [1]. Many experimental studies have shown improved functional outcome after treated with stem cell therapy and transplant [2]. Most of these researches were carried out based on histological evaluations which are time-consuming, tedious, and expensive. Therefore, there is a need for the development of new method to investigate the migration of stem cells in vivo. The understanding of the mechanisms underlying stem cell migration into tissue is an essential step for the development of novel stem cell therapies. Improved stem cell tracking system would also allow evaluating the function and activities of recruited stem cells on the maintenance, repair or replacement of damage tissues [1].

Many methods have been used to track stem cell migration in live animals. These methods include fluorescence labeling, magnetic particles, radionuclides, quantum dots (QDs), and reporter genes**.** Magnetic particle labeling used in magnetic resonance imaging (MRI) involved in using cells tagged with iron oxide nanoparticles that provide great spatial resolution and high sensitivity [3]. Radionuclide imaging techniques, labeling of mesenchymal stem cells with radioisotopes, such as ^{111}In-oxyquinoline, ^{99m}Tc-hexamethylpropylene amine oxime, and also ^{18}F-FDG PET radiotracer, have been used to be the observation of cell targeting [3, 4]. Quantum dots (QDs), is a new fluorescent probe for in vivo imaging with a light-emitting particles on the nanometer scale that improved signal brightness and simultaneous excitation of multiple fluorescence colors [4]. Reporter gene imaging usually encodes specific molecules that interact with imaging probe and generated signal that can be captured within living subjects [3].

1.1 Types of stem cells

Differing from specialized cells (muscle, skeleton, nerve cells, etc), stem cells can proliferate and then differentiate into specialized cells with proper stimulation [5]. It is generally believed that stem cells can be transplanted to repair and to regenerate injured tissue. Such regenerative properties have been widely tested to treat a variety of incurable disease, such as spinal cord injury, Alzheimer diseases, diabetes, etc.

Many sources of stem cells have been used for stem cell therapies. These cell sources include embryonic stem cells, induced pluripotent stem cells, bone marrow stem cells, core blood stem cells, placenta stem cells,..etc.

1.1.1 Embryonic stem cells (ESCs)

ESCs are isolated from embryos at blastocyte stage. It is generally believed that ESCs are pluripotent, highly proliferative, and can differentiate into cells of any types [6]. Despite of their superior plasticity, ESCs have been indicated to promote tumor [7]. In addition, ESCs can only obtain from embryos, vociferous debate continues as to the ethical validity of ESC harvesting [6, 7]. These limitations have substantial hindered the use of ESCs in stem cell therapy.

1.1.2 Induced pluripotent stem cells (iPS)

iPSC are a type of pluripotent stem cell artificial derived from non-pluripotent stem cells (adult specialized cells, such as skin) by up-regulation of a panel of genes, including Oct-3/4, Sox family, Klf family, and c-Myc [8]. iPS cells are similar to ESCs that have the capacity to generate a large quantity of stem cells as an autologous source that can be used to regenerate patient-specific tissues [8, 9]. One disadvantage of iPS is the use of retroviruses [10] that might alteration in genes and cause of many diseases, like cancer [10]. Also, the long-term safety is still unknown and need to be fully investigated.

1.1.3 Adult stem cells

Adult stem cells can be isolated from bone marrow, fat, muscles, and various tissues. Among all sources, bone marrow remains to be the major source of adult stem cells [11]. Bone

marrow fluid and cells are aspiration removes through a needle that injected into a bone. The bone marrow fluid and cells are checked for problems with any of the blood cells made in the bone marrow. Cells can be checked for chromosome problems.

Adult stem cells can be isolated from bone marrow, fat, muscles, and various tissues. Among all sources, bone marrow remains to be the major source of adult stem cells [11]. Bone marrow fluid and cells are recovered using a hollow needles from, typically, the back of the hipbone. The bone marrow fluid contains many cells, including platelets, monocytes, fibroblast, macrophages, and stem cells [5, 6]

There are several types of adult stem cells including: hematopoietic stem cell (HSCs) and mesenchymal stem cells (MSCs). HSCs can be able to renew itself, and can differentiate to a variety of specialized cells that can mobilize out of the bone marrow into circulating blood [12]. MSCs reside within the stromal compartment of bone marrow. With proper stimulation, MSCs can differentiate into other specialized cell types such as osteoblasts, adipocyted, chondrocytes, myocytes, cardiomyocytes, adipose cells, and stromal cells [13]. For stem cell therapy, studies have suggested that bone marrow cells contain neural progenitor cells and can be used for neuronal tissue repairing [14].

1.2 Cell sources for stem cell therapy

Cell therapy involved transplantation, through local delivery or systemic infusion, of autologous or allogeneic cells to restore the viability or function of deficient tissues. A key factor in stem cell-based tissue engineering is the source of stem cells. The source of adult stem cells can be allogeneic (same species, different individual), or autologous [15].

1.2.1 Allogenic stem cells

Allogeneic stem cells are derived from a matched donor (such as a sibling). Traditionally, allogeneic stem cells transplants have been performed using stem cells collected from the bone marrow aspiration, but the use of peripheral blood stem cells is rapidly increasing [16]. However, since the donor and the recipient are different, immunological differences exist [16], including

graft rejection and graft-versus-host disease (GVHD) [17]. The new stem cells may attack the tissues of the patient, but they may also attack the cancer [17].

1.2.2 Autologous stem cells

Autologous transplant means that the transplanted tissue (stem cell) is derived from the person for whom the transplant is intended. The stem cells from the patient's own marrow will "harvested," stored and then returned to the body (engrafted) after the patient receives high doses of chemotherapy and/or radiotherapy conditioning therapy [18]. Autologous stem cells may be collected from the bone marrow by bone marrow harvest. Stem cells are removed from the patient before the treatment and re-implanted afterwards.

Autologous stem cells can be made to not only generate cell types of their tissue of origin but also produce cell types present in other tissues [18]. Ideally, autologous stem cell-derived tissues have almost zero concerns of immune-rejections, thereby avoiding the deleterious side effects of immunosuppressice medications [19].

1.3 Stem cells and tissue engineering

Due to the short supply of viable tissues and organs, tissue engineering has gained popularity as a promising alternative to produce functional organs and tissue for transplantation. The term of “tissue engineering” is defined as “the application of principle and methods of engineering and life sciences toward fundamental understanding of structure-function relationships in normal and pathological mammalian tissue and the development of biological substitutes to restore, maintain or improve tissue function [20, 21].” For a long time, primary cultured cells and cell lines have been used as the main source of cells for tissue engineering. Unfortunately, the potential immune reactions to cell lines and lack of reliable source of primary cells have substantially hindered the potential applications of tissue engineering in medical applications [15]. Due in large part to recent progress in stem cell biology and recognition of the unique biological properties of stem cell, increasing number of tissue engineering studies use stem cells as the major source of cells [22]. Stem cells represent an ideal cell source for tissue

engineering. Since stem cells can be readily isolated, expanded and transplanted, their application in cell-based therapies has become a major focus of research. Biomaterials can potentially influence e.g. stem cell proliferation and differentiation in both, positive or negative ways and biomaterial characteristics have been applied to repel or attract stem cells in a niche-like microenvironment [23].

Although stem cells have been gained their popularity as the main sources of cells for tissue engineering, many limitations have been found to restrict the clinical applications of stem cell-based tissue engineering products. Briefly, the bone marrow aspirate procedure may post risk to some patients and may not applicable to all patients. Despite of excellent plasticity, adult stem cells are hard to grow to sufficient number for soft or hard tissue regeneration. Stem cell culture is time consuming and very expensive. To avoid potential immune rejection, stem cell-based tissue engineering products have to be custom made and cannot be produced in large quantity. Therefore, there is a need for the development of new method for producing stem cell based tissue engineered tissue/organs.

1.4 Stem cells participate in wound healing responses

1.4.1 Role of stem cells in wound healing

In searching for novel method to direct tissue regeneration, we decide to learn from nature tissue regeneration processes - wound healing responses. Wound healing, such as skin injury requires with a complex biological and molecular events of cell migration and proliferation system, as well as extracellular matrix deposition, angiogenesis, and remodeling [24]. During wound healing, stem cells are attracted by inflammatory signals to migrate to the injury site and undergo differentiation promoting structural and functional repair [24, 25]. Stem cells, both mouse and human, have a capacity to differentiate into various tissue types by asymmetric replication, which will help create a complex structure [24].

Many recent studies suggest that inflammatory signals are responsible to stem cell homing to injured tissue [26]. Macrophages, mast cells, neutrophils, and fibroblasts are found to

participate in wound healing responses. Macrophages produce angiogenic factors, proteases and growth factors, which result that stimulates the migration of epithelial-cell, survival and proliferation [27]. The products releases by these inflammatory cells, most notably mast cells and neutrophils, have been associated to the recruitment of stem cells [28, 29]. Some evidences suggest that those recruited stem cells contribute to revascularization of wounds and damaged tissues [24]. Large number of studies has been demonstrated that transplanted marrow-derived stem cells could accelerate revascularization and promote healing at the injured sites [24, 26, 27].

1.4.2 Roles of chemokines and cytokines in stem cell homing

Wound healing responses are always accompanied with the release of a variety of chemokines, cytokines, and growth factors. Many of these factors have been associated with stem cell homing. The specific function of these cytokines and their potential roles on stem cell homing are listed below.

Stromal cell derived-1 alpha (SDF-1α)

SDF-1α, also called as CXCL12a, belong to the group of CXC chemokines. The receptor for SDF-1α is CXCR4 [30]. SDF-1α has been found to express in many tissues, including brain, thymus, heart, lung, kidney, spleen and bone marrow, in mice [31]. In solution, SDF-1α is a potent chemokines for lymphocytes and stem cells [32]. It has also been shown that SDF-1α is critical for bone marrow engraftment as the central signaling axis for stem cell homing and repopulating [32]. SDF-1α plays an important and unique role in the regulation of stem cell trafficking. SDF-1α regulates the homing/retention in major haemato/lymphopoietic organs and accumulation of immune cells in tissues affected by inflammation [33].

Erythropoietin (EPO)

Erythropoietin (EPO) is a release factors from bone marrow derived mesenchymal stem cells (BM-MSCs) that supporting the survival, proliferation and differentiation of hematopoietic stem/progenitor cells [34]. In the presence study has demonstrate the ability of EPO to stimulate

HSC proliferation, and resulting in significantly increased inflammation and ischemiainduced neovascularization [35].

Monocyte chemoattractant protein-1 alpha (MCP-1α)

MCP-1 α is a chemokine, which has been shown to be responsible to the immigration of circulating monocytes to the inflammatory site [36]. It also direct the migration of endothelial cells and T-cells [36], is a potent agonist for monocytes, dendritic cells, memory T cells, and basophils [37], that mediates a remarkably diverse set of effects in different disease models. It has been shown that MCP-1α can enhance the recruitment of stem cells to specific sites [38].

Macrophage Inflammatory Protein-1 alpha (MIP-1α)

MIP-1α, a potent inflammatory chemokines, has been shown to play an important role of chronic inflammatory responses [39]. Recent studies have also uncovered that MIP-1α triggers the migration of bone marrow stem cells, both MSCs and HSCs [39]. In addition, MIP-1α is also known as an inhibitor of the proliferation of particular populations of stems cells, which can transiently engrafting hemopoietic stem cells to stimulate the recruitment of stem cell homing [39].

Chemokines are known to direct immune cells to sites of inflammation, which regulate proliferation and migration of various types of normal stem and progenitor cells. Based on this, it is conceivable that the established role of chemokines in stem proliferation and recruitment might also be associated with inflammatory response.

1.5 Recent development of *in vivo* cell tracking technology

To examine cell migration *in vivo*, most of the research relies on histological evaluation of tissue samples. Histological evaluation (sectioning and staining) requires large number animal cohorts as multiple animals at each time point and long time for measurable changes to occur for the histology study [40]. In addition, histology evaluation provides semi-quantitative 2-dimensional data and may not provide the overall 3-dimensional distribution of the cells in tissues. To solve such problem, many imaging methods have been developed to localize and tracking numbers of engrafts stem cells, including magnetic resonance imaging (MRI), and x-ray

computed tomography (CT) [41, 42]. Several studies have been using MRI imaging or CT to track transplanted stem cells by labeled with MR contrast agents [43]. These techniques offer high resolution, but can constrained by sensitivity and high cost [42, 44]. Optical methods typically offer a higher sensitivity for monitoring compare to MRI, CT [45], and are relatively inexpensive [45]. Specifically, many florescence-based on small animal *in vivo* Imaging System has recently been developed for efficient tracking of labeled cells, and evaluated the delivery and regenerative potential by adding the X-ray imaging system that improved data by using the live animals for continued studies [40, 43].

Many cell-labeling agents have become available for tracking cell migration in vivo. These cell-labeling agents are quantum dot-based (Qtracker®), and near infrared dye based (X-Sight Quantum dots, an optical property that conjugated probes to specific biomarkers have specific wavelength of their fluorescence depend strongly on their size [45]. It is a suitable fluorescence probes for all types of labeling studies due to the reduced of tendency to photobleach [45], and can be applied in a multiplex manner to single tissue sections of biopsies to measure expression levels of multiple biomarkers [46]. However, quantum dots contained with heavy metals, which are potentially toxic to organisms over long times [46]. Also, the dots are larger and not always taken up by some cells, like bacteria [47]. The near infrared (NIR) dye based (X-sight) is a novel line nanospheres of organic fluorescent nanoparticles, which offer superior brightness, photostability, and biocompatibility for *in vivo* image tracking [41]. They can also be used to label a variety of cells. Most importantly, following transplantation, NIR-labeled cells can be monitored in real-time [41].

Despite of such progress made in recent years, imaging tool has not been used to monitor the recruitment of stem cells response to tissue scaffolds *in vivo*. Since our long term goal is to develop degradable tissue engineering scaffolds to recruit stem cells, it is essential that an *in vivo* imaging method is developed to monitor stem cell migration. For that, this study is aimed at developing and then using *in vivo* imaging method to track and to identify the

localization *in vivo* of the transplanted stem cells to the site of injury after different routes of injection at different time points.

CHAPTER 2

OVERALL HYPOTHESES

Most of stem cell-based tissue engineering requires the scaffolds to be pre-seeded with stem cells prior to transplantation. Unfortunately, the transplanted stem cell-seeded scaffold often failed to survive *in vivo* due to lack of required vascularity, and did not support enough mechanical strength for cells to grow [23]. To combat such challenge, our long term goal is to develop tissue scaffolds which can recruit and then differentiate autologous stem cells. Our recent studies have accidentally discovered that biomaterial implantation prompted the recruitment of autologous stem cells. Based on many others and our results, we found that inflammatory products may be responsible to stem cell migration. Furthermore, the numbers of recruited stem cells may be increased with localized delivery of stem cell chemokines. Finally, scaffold surface functionality has been shown to affect the extent of foreign body reactions. It is likely that material surface chemistry may also influence the degree of stem cell recruitment. My research was aimed at testing the following three hypotheses.

2.1 Hypothesis I

Localized inflammatory responses are responsible to the recruitment of stem cells.

2.2 Hypothesis II

Locally released stem cell chemokines enhance stem cell immigration to tissue scaffold.

CHAPTER 3

INFLUENCE OF INFLAMMATORY RESPONSES ON STEM CELL RECRUITMENT (HYPOTHESIS I)

3.1 Rationale

Following implantation, all biomaterials prompt different extent of foreign body reactions, accompanied by the accumulation of large of inflammatory and fibrotic cells [48]. A variety of cytokines have been uncovered to play an important role of foreign body reactions. Briefly, chemokines and their receptors can direct the movement of mononuclear cells throughout the body, engendering the adaptive immune response and contributing to the pathogenesis of a variety of diseases [37]. Studies have shown the migration of phagocytes toward implant surfaces had up-regulation of message of MCP-1α and MIP-1α [48, 49].

Interesting, many of these inflammatory cytokines/chemokines have also been implicated in recent work to promote stem cells recruitment. Specifically, MIP-1α is a chemokines that primarily associated with cell adhesion and migration. Several chemotaxis studies showed that MIP-1α expressed significant activity towards bone marrow cells that restored the osteoclast progenitors back to the normal level, which suggested that MIP-1α involved in migration of bone marrow stem cells [39, 50]. MCP-1α is known as attracting monocytes to sites of inflammation. It has been successful reported that the stimulated with MCP-1α would activated the migration capacity of rat-derived neural stem cells compared to the untreated one [50]. Since SDF-1α plays an important role in the homing of stem cells to the injured tissues, it is also involved in the recruitment of inflammatory cells and other types of stem cells [51-53]. The dual function of these chemokines made us to assume that the degree of biomaterial-mediated inflammatory responses also influences the extent of stem cell recruitment.

Several studies have been able to demonstrate the migration capacity of stem cells in rat and mouse, but the major challenge for the development and refinement of stem cell transplantation is to map the spatial distribution and rate of migration *in situ*. Most imaging systems provide 2-dimensional (2D) information in rodents, showing the locations and intensity of light emitted from the animal in pseudo-color scaling [41]. A live 3-dimensional (3D) capability for imaging tracking is now routinely applied to serially detect the location, identify and measure the number of stem cells [41]. For this reason, among the various imaging modalities that have been developed, in this type of investigation, including X-ray [54], Magnetic resonance imaging (MRI) [55], bioluminescence imaging (BLI) [42] and fluorescence imaging [45] provide means of tracking transplanted cells *in vivo*. Those techniques offer both near-infrared resolution and whole-body imaging capability [42, 54, 55]. Despite those visualization techniques, fluorescence imaging is emerging as an important alternative because of its operational simplicity, safety, and cost-effectiveness [54]. This technique offers the promise of non-invasively quantifying and visualizing specific molecular activity in living subjects in three dimensions [54].

3.2 Materials and methods

3.2.1 Materials

Dulbecco modified Eagle medium (DMEM) was purchased from (Sigma, St. Louis, MO). Fetal bovin serum (FBS) and antibodies against (Penicillin-Streptomycin) were purchased from (Atlanta, Lawrenceville, GA), respectively. Complete medium (90% DMEM, 20% FBS, and 1% antibodies) was prepared as described previously [56]. Trypsin were purchased from (Sigma, St. Louis, MO) and dissolved in phosphate-buffered saline (PBS) (8 mg NaCl, 0.2mg kH_2PO_4, 1.56mg Na_2HPO_3, 0.2mg KCl, pH 7.2) in 2.5mg/ml, respectively.

3.2.2 Production of polylactic acid particles.

To simulate foreign body reactions without triggering significant surgical trauma, polylactic acid (PLA) particles were produced and used for implantation. Particles were prepared according to a modified precipitation method and were synthesized in our laboratories. The

starting procedure was as follows. PLA polymer (0.2g) was dissolved in 2ml Dichloromethane (DCM). The organic phase was added dropwise into the aqueous PVA phase (20 ml) and stirred magnetically at room temperature until complete evaporation of the organic solvent DCM had taken place. The suspension was then transferred to centrifuge tube and centrifuge (Beckman) at 3000 rpm for 15 minutes. The supernatant was collected and the pellet freeze-dried for calculating the loading efficiency. Then the pellet was resuspend in 10ml PBS and vortex for 1 minute. The resulting solution was freeze at -80^{0}C and then freezes dry to get the particles.

3.2.3 Bone marrow MSC culture

Isolation of BM MSCs was carried out following established procedures [56]. Balb/c mice were used as donors in all experiments. Both the femurs from Balb/C mice (12 to 20-weeks old) was excised with a scissor removing, and carefully cleaned to remove the adherent muscle tissue. Bone marrow cells were obtained by inserting a syringe needle (25-gauge) and flushing with DMEM containing 20% FBS. The cells were dispersed and suspended with the same medium for several times. Then the marrow cells were plated onto 25-cm^2 plastic flasks (containing 1x10^6 to 2x10^6 marrow cells) with 8ml complete medium, and incubated in a fully humidified system containing 95% air and 5% CO_2 at 37^{o}C. After 3 to 4 days by when cells had attached, the non-adherent cells were removed by changing the culture medium. When primary stem cells formed a cell layer in culture flasks, the cells were subculture into 75-cm$_2$ plastic flasks by using 0.025% trypsin. The cells were passaged two to four times, and then harvested for the *in vitro* and *in vivo* study.

3.2.4 Cell labeling with imaging agent

To determine cell labeling efficacy *in vitro*, cultured stem cells were seeded in 6-well plates (Corning Costar, Corning, NY) in DMEM with 20 % of FBS. When the cells reached confluence, medium was replaced with fresh culture medium with various concentrations of Kodak X-Sight imaging agent (0.1 uM to 0.5 uM, 1457068, Rochester, NY) in each well-plated and cultured at 37^{o}C for 24 hours. Cells were then washed with PBS twice to remove excess

imaging agent followed by analysis with Kodak *In-vivo* Multispectral Image System FX (configured for 760nm excitation, 830nm emission, 60s exposure, f-stop 2.5, 120mm field of view).

To determine the relationship between fluorescence intensity and cells number in tissue, we used MSCs labeled with both Kodak X-sight imaging agent and CFDA-SE (carboxyfluorescein diacetate succinimidyl ester). Kodak X-sight label can be quantified using *in vivo* imaging system. On the other hand, cell labeled with CFDA-SE can be identified in tissue section. Such information can be used to estimate the numbers of immigrated MSCs in the tissue. CFDA-SE is a fluorescent labeling dye with great cell compatibility and commonly used for labeling and tracking cell migration and location [52, 57]. This fluorescent dye with an esterifies form readily passes though the cell membrane of viable cells. Upon entering the cell, they are hydrolyzed by intracellular esterase producing polar fluorescent molecules that are retained in the cytoplasm [58].

A stock solution of CFDA-SE was prepared by dissolving a 0.5-mg vial in 90ul of dimethyl sulfoxide (DMSO) (invitrogen). A labeling solution was then prepared by mixing 2uM stock solution with 6ml Phosphate-buffered saline (PBS). The X-Sight containing medium was removed from the flask and the prepared CFDA-SE solution was added. Cells were incubated for 15 minutes at 37^{o}C to label live cells (green) [42]. Then the double labeling stem cells were washing with PBS twice to remove the dead cells, trypsinzed, and centrifuged twice to wash away the excess labeling agent and trypsin. The total cell number was calculated using hemocytometer.

3.2.5 Animal model and in vivo cell tracking system

To trigger localized inflammatory responses, a subcutaneous PLA particle implantation model was used [52]. In brief, after ventral skin depilation and anesthesia, 0.5 ml of PLA particles was then injected subcutaneously on the lower back-side of Balb/c mice (12 to 20 weeks old). For implantation, mice were anesthetized with isofluorane and the incision site marked and

disinfected with 70% ethanol. Simultaneously, cultured MSCs were incubated with 12ml of complete culture media within 5uM solution of Kodak X-Sight imaging agent at 37^0C for 24 hours. After particle implantation for 24hours, X-Sight labeled stem cells ($3x10^6$/0.2ml) were injected via a 25-gauge syringe needle intravenously (IV) and intraperitoneally (IP) into the individual animals.

After implantation for different periods of time, stem cells distribution was then imaged by using Kodak *In-vivo* Multispectral Image System FX (configured for 760nm excitation, 830nm emission, 45s exposure, 8x8 binding, f-stop 2.5, 120mm field of view) and followed by with X-ray image capture to determine stem cells fluorescence intensity, and stem cell migration. The overall fluorescence intensity images of abdomen and implantation sites vs. time ware analyzed by using Kodak *In-vivo* imaging system at various time points. The high resolution images will be detected by the fluorescent signals emitted by the X-Sight imaging agents. Also, the X-rays were differentially absorbed by bone and soft tissues, creating a projection of the mice's anatomical structure on the phosphor screen [40]. The software of overlay fluorescence and X-ray images of the mice with Intraperitoneal (IP) and intravenously (IV) injection with/without implantation are designed by our lab, which demonstrated the expected colocalization and the precise localization of the labeled cells distribution at various times under the same condition.

3.2.6 Histological evaluation

To visualize and to quantify the numbers of recruited MSCs, histology work was done on some implants and surrounding tissues. At the end of the experiments, animals were sacrificed by CO_2 inhalation and implants and surrounding tissue were be taken out and embedded in a plastic mold in freezing medium OCT (Optimum Cutting Temperature). The molds were placed in a cryostat (Leica, Wetzlar, Germany) and allowed freeze overnight [20, 52]. Then the implant were sectioned in the cryostat with 12um thickness, and collected on poly (l-lysine) treated positively charged slides for histological and immunohistochemical staining and cell density analyses.

To determine of the extent of inflammatory response to PLA implant, some slides were stained with Hematoxylin and Eosin Y (H&E stain, Sigma, St. Louis, MO) according to the manufacturer's instructions. CFDA-SE stains were done to determine and identify what types of recruited cells. Stained sections were visualized using a Leica microscope and imaged with a CCDamera (Retiga EXi, Qimaging, Surrey BC, Canada). The measurements of tissue thickness and cell densities at the material: tissue interface were then performed in Image J [52]. The average of density and thickness of the capsular were measured and collected from H&E stained cross-sections of the implant and surrounding tissue, with images captured on the skin side of the biomaterial interface.

To visualize CFDA-label cells, the implantation site sections were fixed with cold methanol for 10 min, rinsed with PBS for twice, then the sections were staining with 4′,6-diamino-2-phenylindole dihydrochrolide (DAPI) (Invitrogen; Carlsbad, CA) to stain cell nuclei for 5 minutes and rinsed with PBS twice. Stained sections were visualized by using a Leica microscope equipped with a CCD camera (8.4V, 0.9A, Nikon Corp., Japan). Two-dimensional images of each section were then taken using a 20X objective, and stacked using Image J. Each section was then scanned using the particle counter. The particle counter settings were adjusted to account for only a specified range consistent with stem cells sizes determined by measuring the maximum pixilated area of individual cells on the PLA implant sections. Data for physical cell number counts were acquired for each section and compared with fluorescence intensity to verify correct correlations.

3.2.7 Statistical analyses

One-way analysis of variance (ANOVA) was used to compare groups ($p<0.05$). Afterward, Student t-tests were used to compare each method, with

surface seeding assigned as control with Bonferroni adjustment ($p<0.05$).

3.3 Results

3.3.1 In vitro labeling of MSCs

The efficacy of X-Sight imaging agent for labeling bone marrow MSCs was tested *in vitro.* After incubation with different concentrations (1uM, 2uM, 3uM, 4uM, 5uM) of X-sight for 24 hours, the cells were washed with PBS twice and then the fluorescence intensity of adherent cells were determined using Kodak imaging system (Figure 1a). Our results have shown that the fluorescence intensity increased as the concentration increased (Figure 1b). The highest fluorescence intensity was found to associate with cells incubated with X-Sight at 5uM/2ml complete medium (Figure 1b), while the unlabeled cells did not exhibit any detectable fluorescence. Based on the results of this work, in later study, MSCs labeling was carried out by incubating cells with X-Sight at 5uM/10ml complete medium. The higher the concentrations of X-Sight were used to label cells, the stronger the cell-associated fluorescence intensity (Figure 1b).

To further characterize this result, all the MSCs were labeled with X-Sight (5uM/10ml complete medium), and initial cell labeling efficiency was determined using Kodak *In-Vivo* system 24 hrs after labeling. Unlabeled cells exhibit minimal or no background fluorescence inside 25-gauge syringe needle (Figure 2). However, intensive fluorescence can be seen on X-sight-incubated MSCs. This process is used to confirm the success of labeling each time prior to all *in vivo* experiment. In addition, this in vitro measurement also allows us to quantify the fluorescence intensity per numbers of cells.

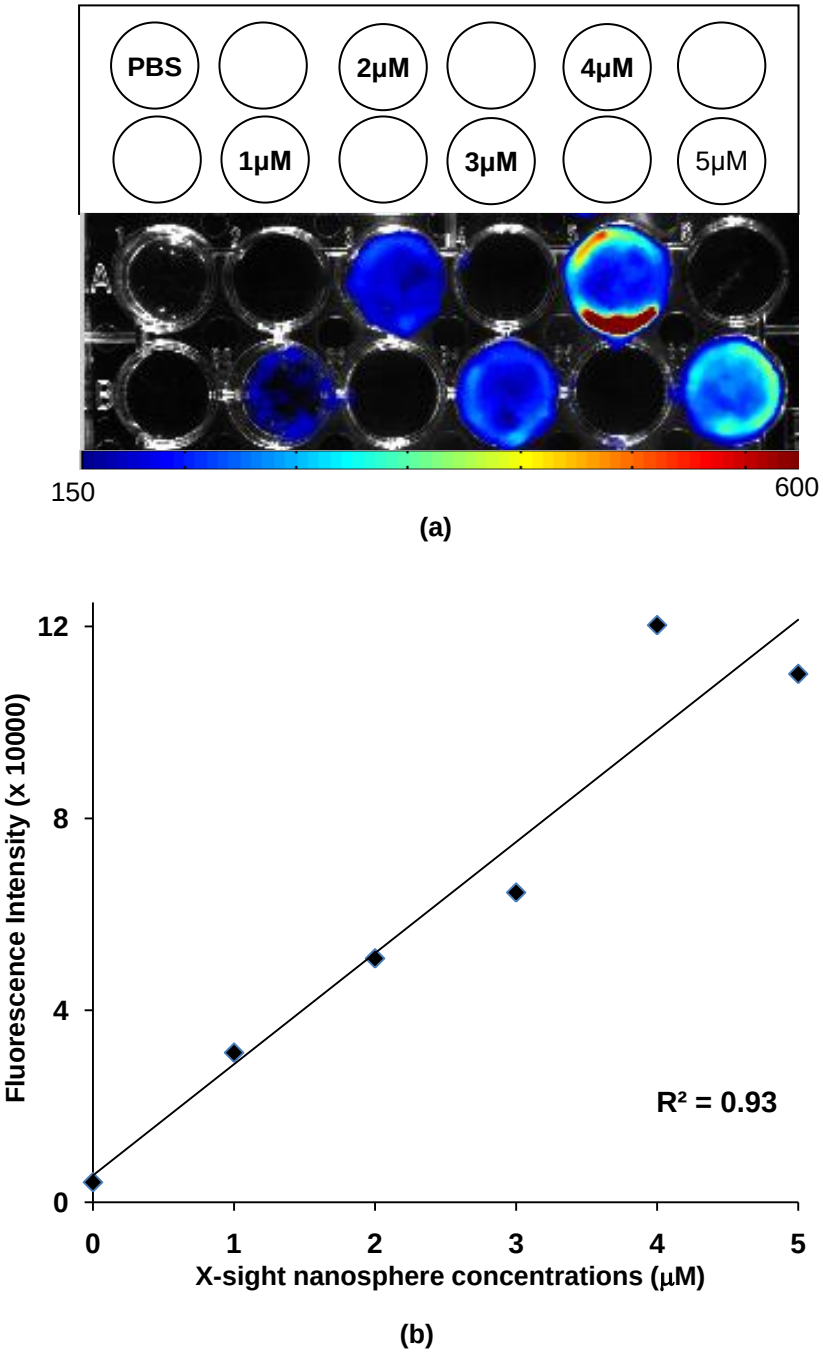

Figure 1 In vitro Imaging of MSCs labeled with NIR X-Sight Nanospheres. (a) Well plate fluorescence image of stem cells ($4x10^6$ cells in each well) incubated with different concentrations of X-Sight (from left to right: PBS, 1μM, 2μM, 3μM, 4μM, and 5μM) (b) The correlation between cell-associated fluorescence intensities and NIR agents labeling concentrations is determined.

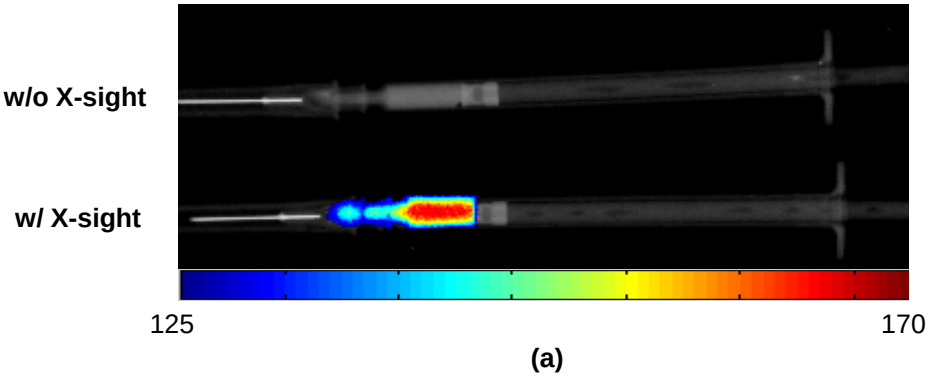

(a)

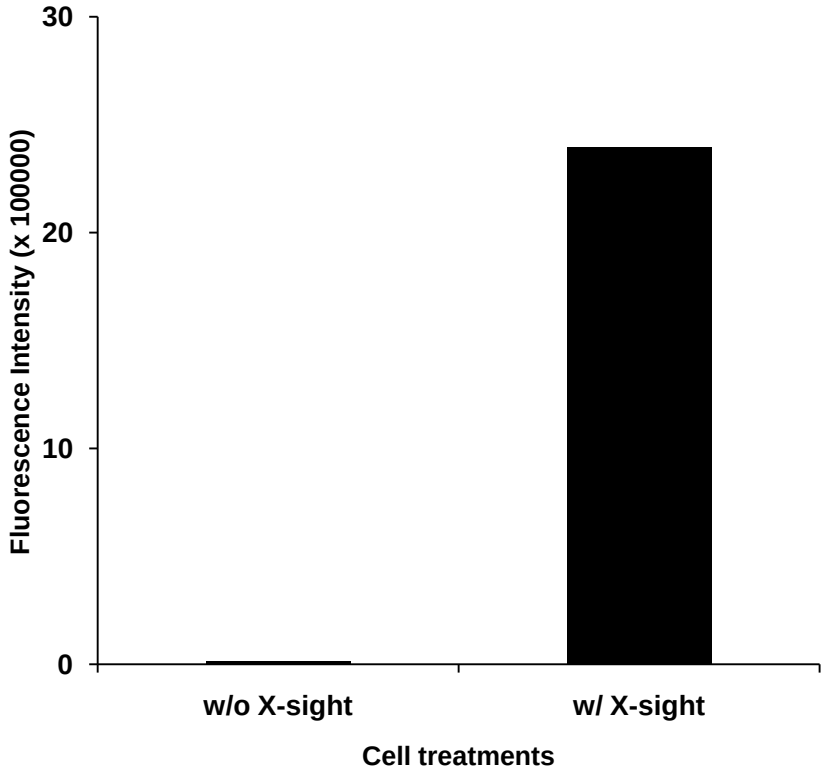

(b)

Figure 2 (a) *In vitro* images of labeled MSCs inside 25-gauge syringe needle (upper needle: MSCs without labeling served as background; lower needle: MSCs labeled with X-sight) (b) The fluorescence intensity of labeled MSCs and non-labeled MSCs can be quantified.

3.3.2 Effects of inflammatory responses on stem cell recruitment in vivo

In order to determine whether labeled cells can be monitored with *in vivo* imaging system, mice transplanted intraperitoneally with un-labeled stem cell were imaged. As expected, we found that there was no detectable signal appearing on both anterior and dorsal side after cell transplantation for 0hr, 24hr, and 48hr (Figure 3a). However, after transplanted with X-Sight-labeled stem cells in the intraperitoneal cavity for 0hr, 24hr, and 48hr, strong fluorescence was found at the ventral (transplanted) side of the animals (Figure 3a). Interestingly, we find that there was no signal from the dorsal site (Figure 3b). These results suggest that most of the transplanted MSCs stayed in the peritonea cavity with very little or no cell migration. To test the influence of inflammatory responses on MSCs migration *in vivo*, mice were implanted with PLA particles at the front back side of the mice. It is well established that PLA particles prompt localized inflammatory responses in the implantation site. After PLA particle implantation for 24 hours (which are the time required for maximal inflammatory responses), X-Sight labeled MSCs were injection at the intraperitoneal space, which is far away from the inflamed tissue on the back of the mice. Mice without PLA particle implantation were also used as a control. Figure 4 shows that, shortly after cell transplantation, majority of the MSCs were present in the peritoneal site (Figure 4a). Twenty four hours later, lesser fluorescence intensity was found in the ventral position. On the other hand, fluorescence increased on the dorsal area of mice nearby the particle implantation site (Figure 4b). These results suggest that substantial number of MSCs migrated from the implantation site (peritoneal cavity) to the particle implantation site, area with localized inflammation. Such cell migration was not found in mice without PLA particle implantation (Figure 4b). There is, however, a slightly decrease of fluorescence intensity at 48 hours indicating that some of immigrated MSCs left the implantation sites (Figure 4b).

In previous studies, PLA particles were implanted in the dorsal neck area. However, we have also observed that the fluorescence background signals in the neck area have high background sometime (Figure 5). Such high background fluorescence signals around the neck

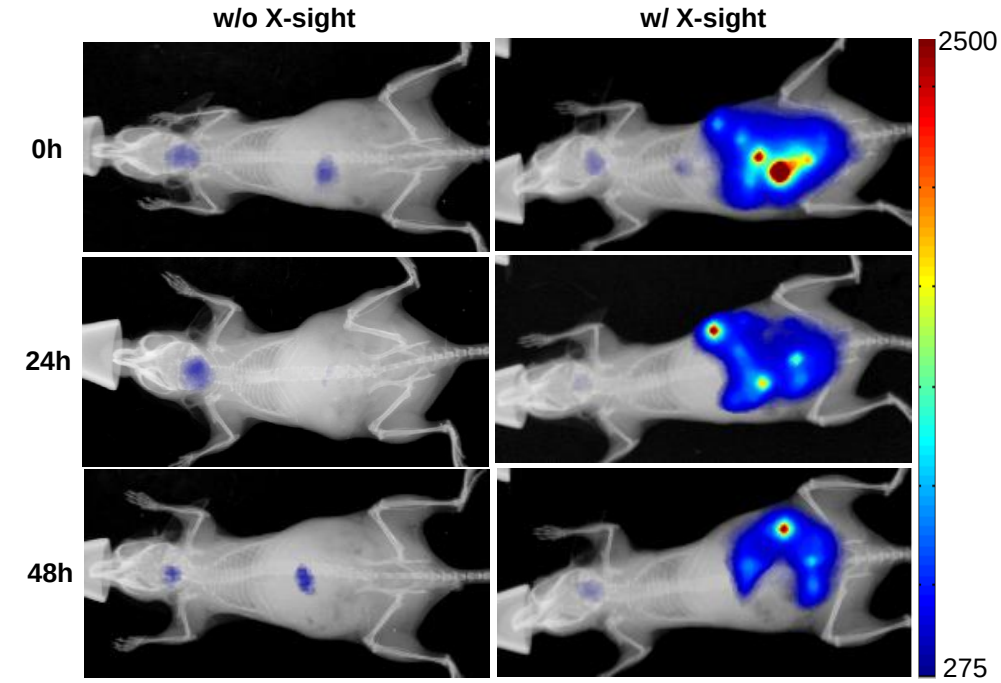

(a) Ventral

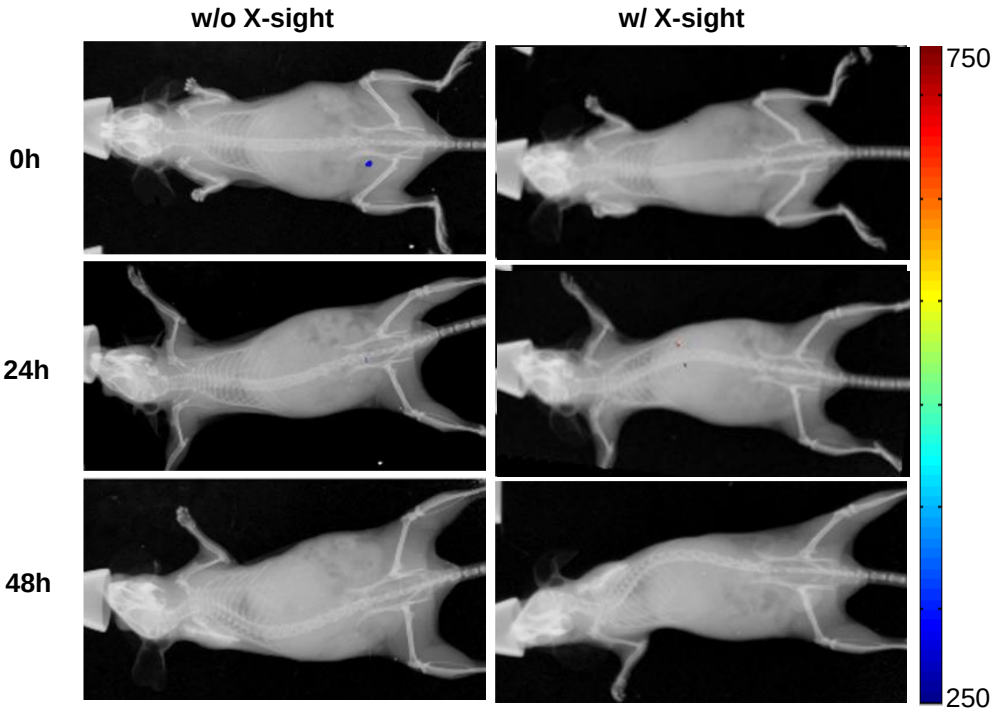

(b) Dorsal

Figure 3 *In vivo* images of transplanted MSCs into the intraperitoneally sites of mice with and without X-Sight-labeling at 0h, 24h, 48h (from top to bottom).. (a) Mice imaging at dorsal position. (b) Mice imaging at ventral position. (L: MSCs without labeling, R: MSCs labeling with X-sight)

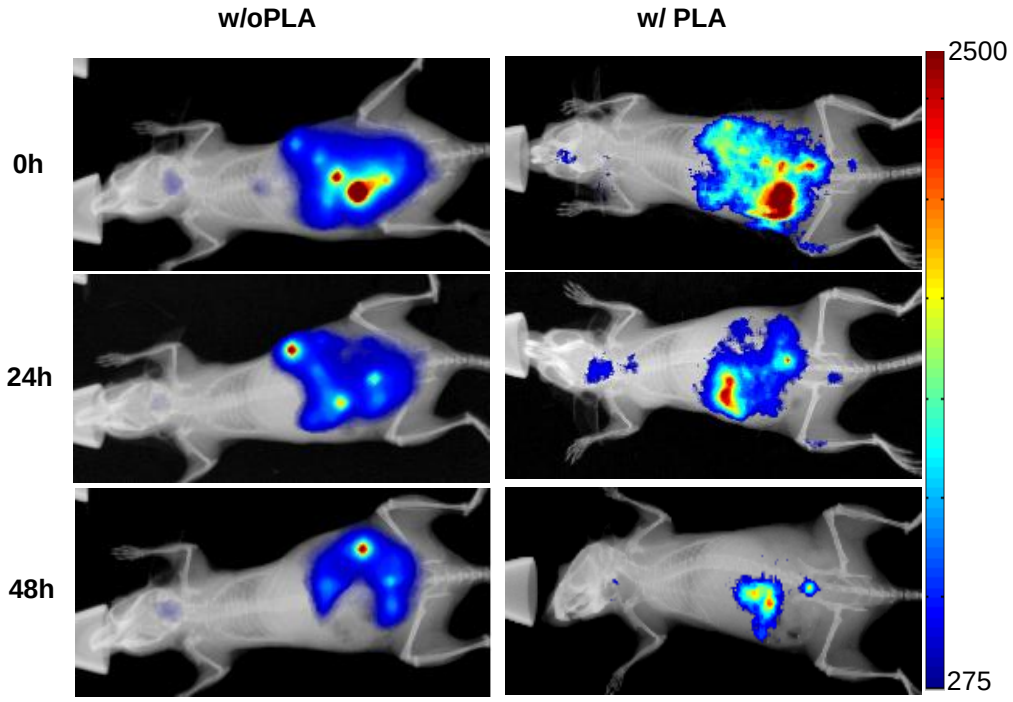

(a) Ventral

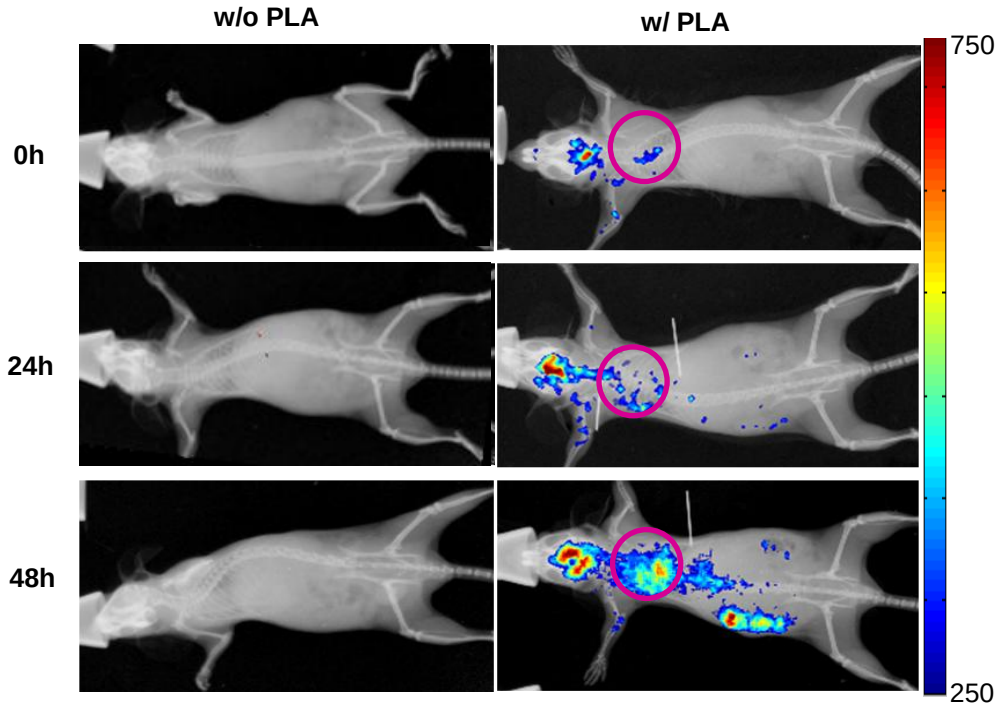

(b) Dorsal

Figure 4 The comparison of mouse with PLA implant and without at 0h, 24h, 48h (from top to bottom). (a) The signal intensity of IP site at. Left is the mouse with PLA implantation, and the right one is without PLA implantation (Ventral). (b) Mouse signal in the implantation site (Dorsal). ◯: Implantation area.

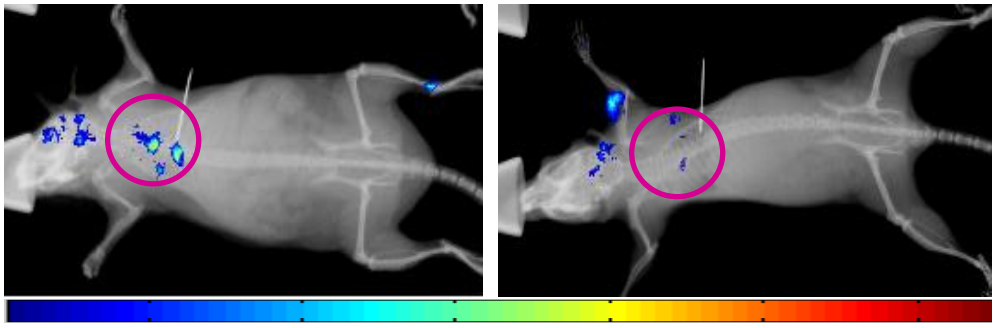

Figure 5 The fluorescence background signals in the area behind the neck are not very consistent. However, the lower dorsal back area consistently has lower fluorescence. ○: Implantation area.

area might be associated the inability to remove all fur prior to imaging. On the other hand, we have noticed that the tissue nearby the lower back area has consistently lower fluorescence background. Therefore, in the following studies, all particle implants were implanted subcutaneous in the low back of animals.

3.3.3 Correlation between in vivo fluorescence intensity and cell numbers

The previous results were base done solely fluorescence intensities with the assumption that there is a good relationship between fluorescence intensities and stem cells numbers in tissue. To test this hypothesis, two series of studies were carried out.

First, using subcutaneous implantation model, different numbers ($2x10^4$, $5x10^4$, $1x10^5$, $2x10^5$, $5x10^5$, and $1x10^6$) of X-Sight labeled MSCs were injected subcutaneously on the back of mice. The fluorescence intensities on different sites were measured (Figure 6a). The florescence intensities were then correlated with the known cell numbers. The results (Figure 6b) show that there is an excellent correlation (R^2= 0.99) between fluorescence intensities and MSCs numbers in subcutaneous space.

Second study used MSCs doubled with X-Sight and CDFA-SE. The double stained cells were transplanted into the peritoneal cavity of mice implanted with PLA particles. Forty-eight

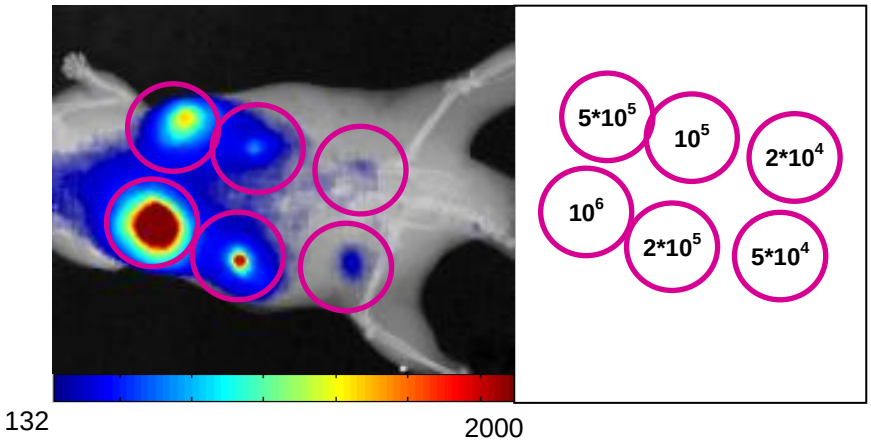

(a)

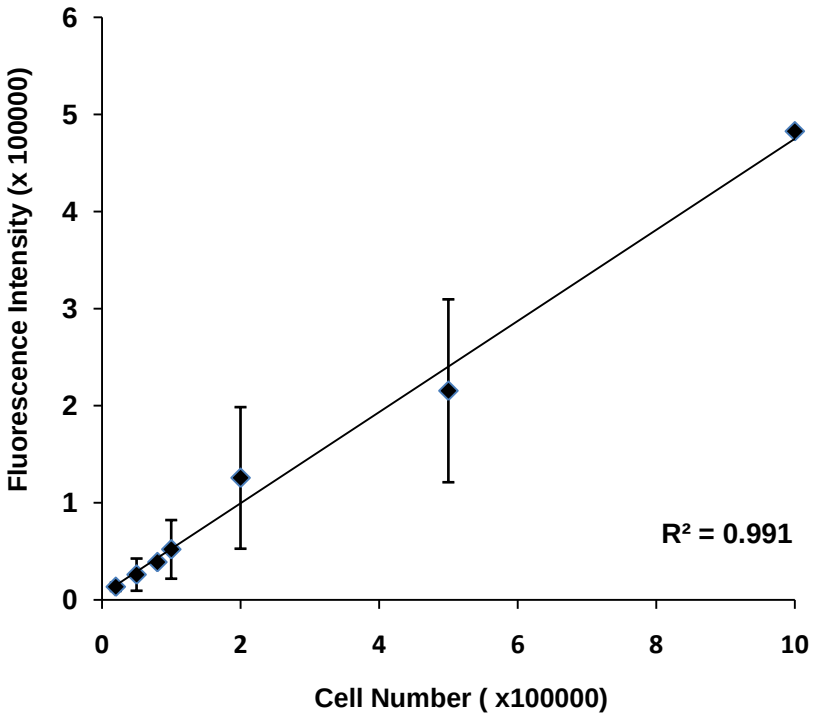

(b)

Figure 6 In vivo quantification of stem cells. (a) $2*10^4$, $5*10^4$,10^5, $2*10^5$,$5*10^5$, 10^6 stem cells labeled with X-sight and directly imaged after injection. (b) Fluorescence integrated intensity recorded in the regions were plotted, after subtraction of background, versus the numbers of stem cells. ○: Implantation area.

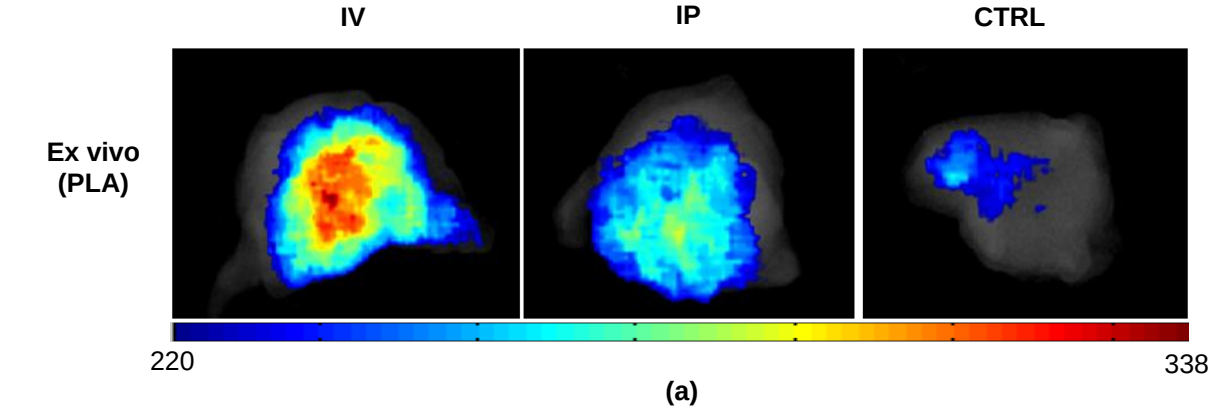

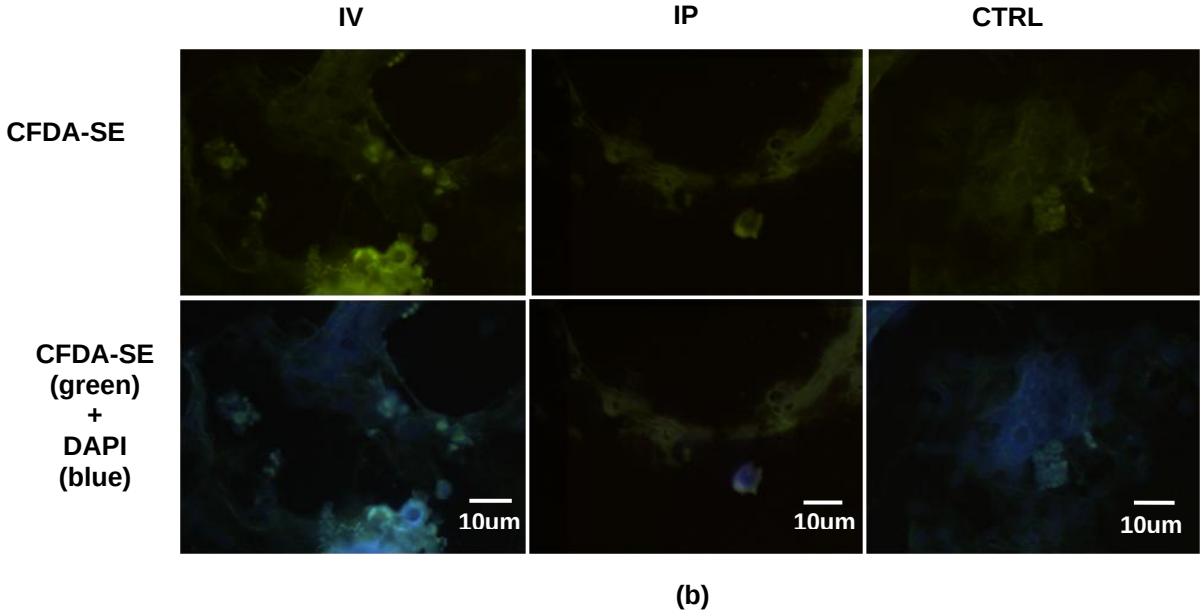

Figure 7 (a) The microscopy Imaging of transplanted MSC migrate to the PLA implantation site after 48hrs implantation by using CFDA-SE double staining, from left to right: IV injection, IP injection and another IP injection experiment (without labeling X-sight as control). (a) The ex vivo PLA implantation imaging results. (b) PLA implantation site frozen section, green signal shows CFDA-SE labeled MSCs, and the blue signal shows DAPI staining.

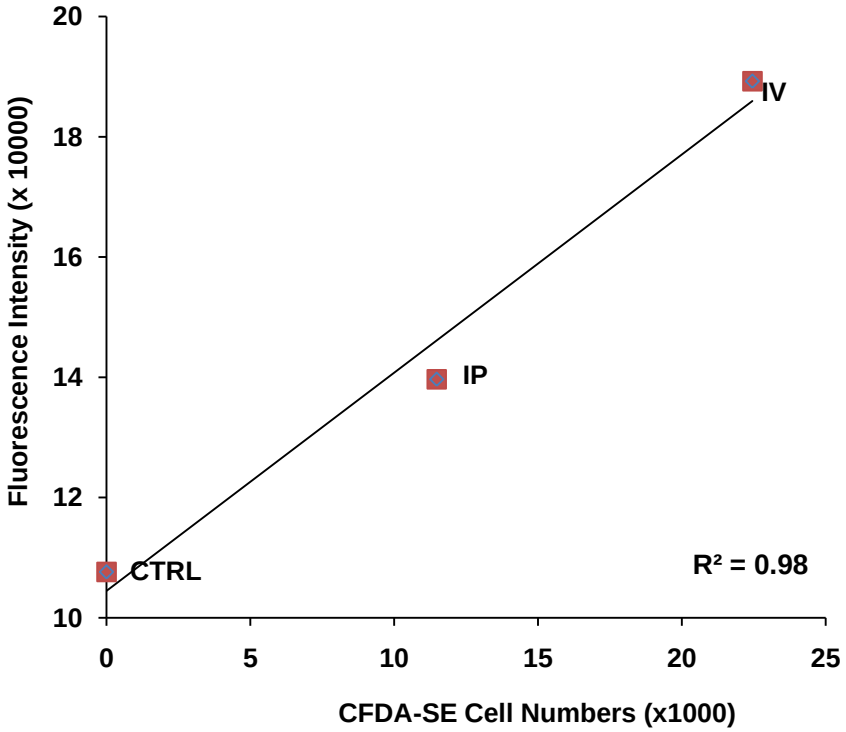

Figure 8. The correlation between intensity counts and numbers of MSCs expressing CFDA-SE transuded.

hours following cell transplantation, the *ex vivo* fluorescence imaging and intensity can be determined using imaging system (Figure 7a). The implant-surrounding tissue were isolated, and then frozen sectioned. The numbers of immigrated CFDA-labeled MSCs can then be quantified, since the presence of CFDA-SE labeled cells can be visualized under fluorescence microscope (Figure 7b). The correlation between in vivo fluorescence intensity and histology cell counts was determined (Figure 8).

Overall our results have shown that subcutaneous cell transplantation model gave us the best relationship between cell numbers and fluorecence intensities. On the other hand, CFDA-labeled MSCs were difficult to be identified in tissue due to low cell numbers. Although there is a reasonable correlation between CFDA-labeled MSCs numbers and fluorescence, the

variations of the results within the same treatment group are large. Therefore, in the future study, the cell quantifications were carried out based on the relationship generated using subcutaneous cell transplantation model.

3.3.4 Influence of the transplantation sites (Intravenous vs. intraperitoneal) on MSCs migration

To the best of my knowledge, no study has been done to compare the responses of MSCs transplanted in the intraperitoneal vs. intravenous space. To study the effect of transplantation sites on MSCs migration, X-Sight labeled MSCs were administered into intraperitoneal or intravenous space and the biodistribution of MSCs were then monitored using imaging system. Since inflammatory cells are the major component of the capsule surrounding biomaterial implants, switching the implantation site should be elicit the same stem cell recruitment. Indeed, the labeled stem cells with IV injection was found to have signal intensity increasing through time point at the IP cavity, and decreasing with IP injection (Figure 9). As expected, both IV-administered and IP- administered MSCs were found to migrate to the PLA particle implantation sites (Figure 10a&b). On the other hand, when cells were transplanted in the IP cavity, we saw the reduction of the fluorescence intensity in IP with time indicating the emigration of MSCs (Figure 10b). Based on the in vivo images, we also notice that a very few MSCs were found in the ventral space following IV transplantation (Figure 9a).

Interestingly and rather unexpectedly, by compared results between IP and IV administration, we observed that more cell immigration into PLA implantation site when the MSCs were transplanted into intravenous space than peritoneal cavity (Figure 10c). Although the cause(s) for such cell response difference has yet to be determined, we believe that most of intraperitoneally injected MSCs were stayed in the peritoneal space and only part of the intraperitoneal transplanted MSCs entered the circulation and then reached the PLA particle implantation site. On the other hand, all of intravenous transplanted MSCs were in the circulation and have had better chance to reach the PLA implantation site.

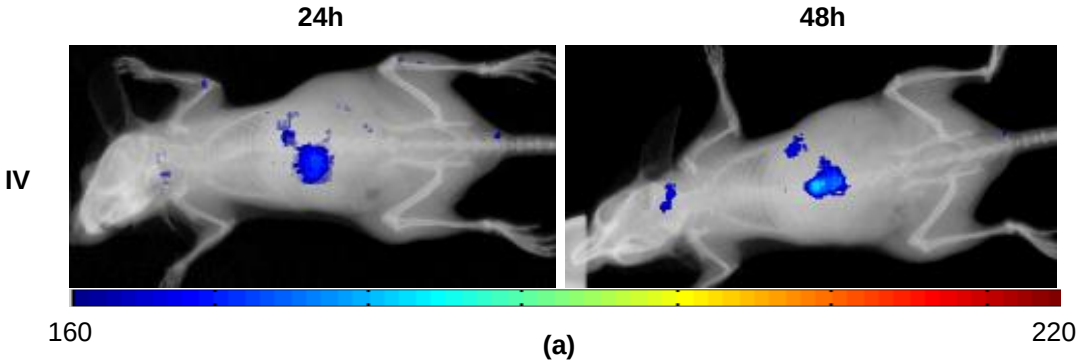

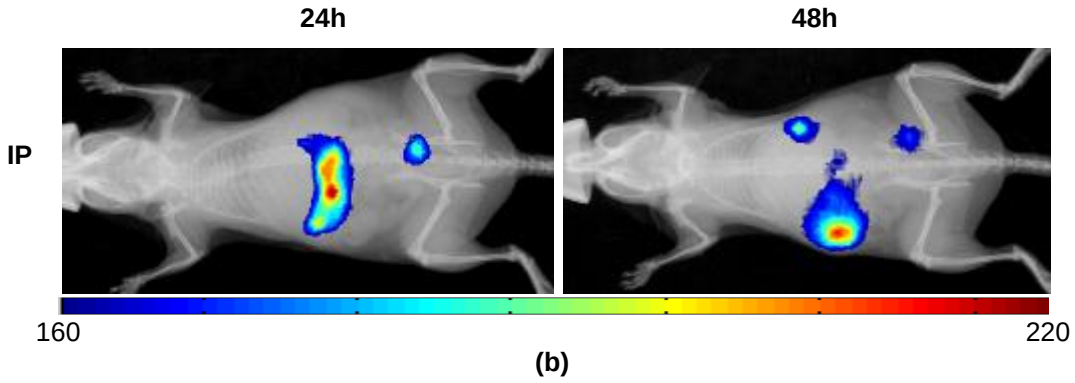

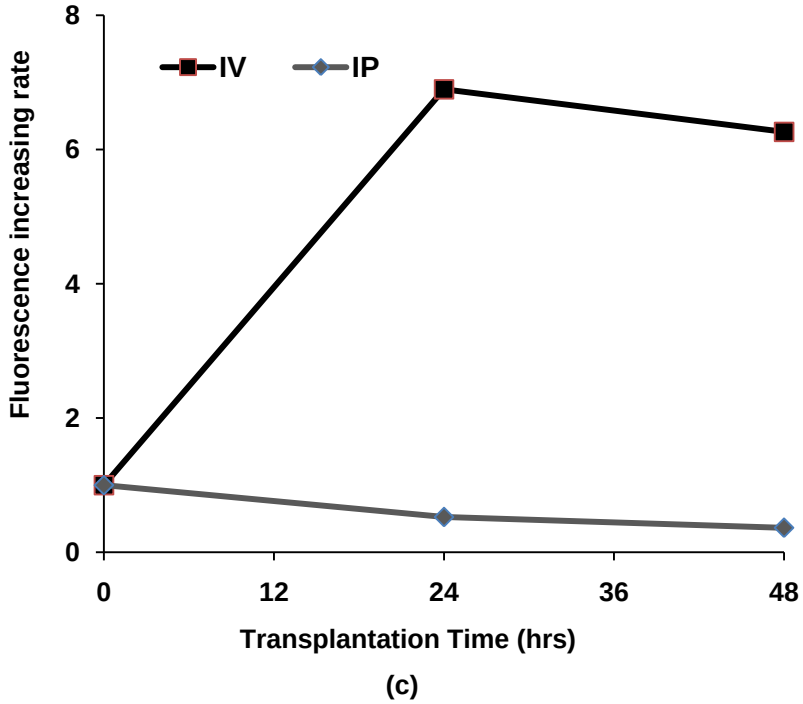

Figure 9 Examination the distribution of MSCs using whole-body imaging system. Time points examined between the peritonea cavity fluorescence intensity with IV (a) and IP (b) injection with 24h, 48h (from left to right).(C) The signal intensity of IP site with IP injection was decreasing through time points.

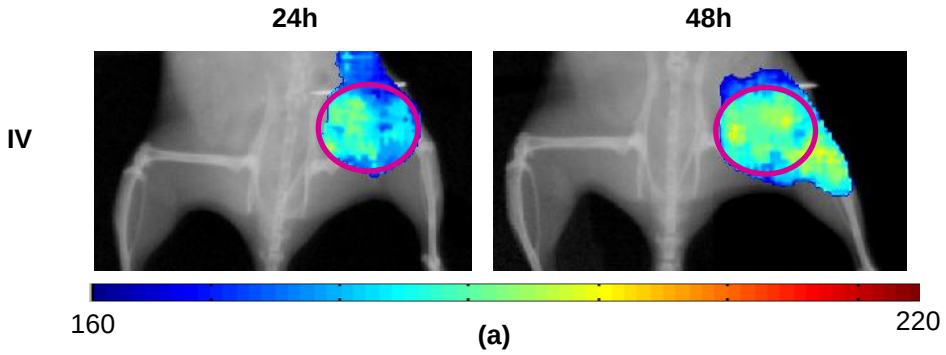

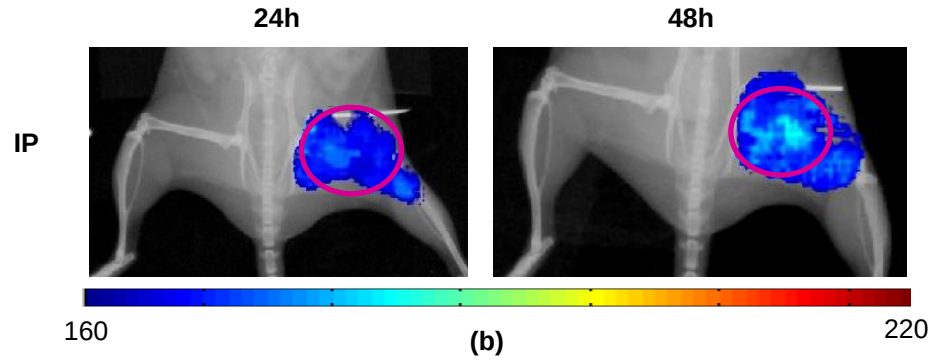

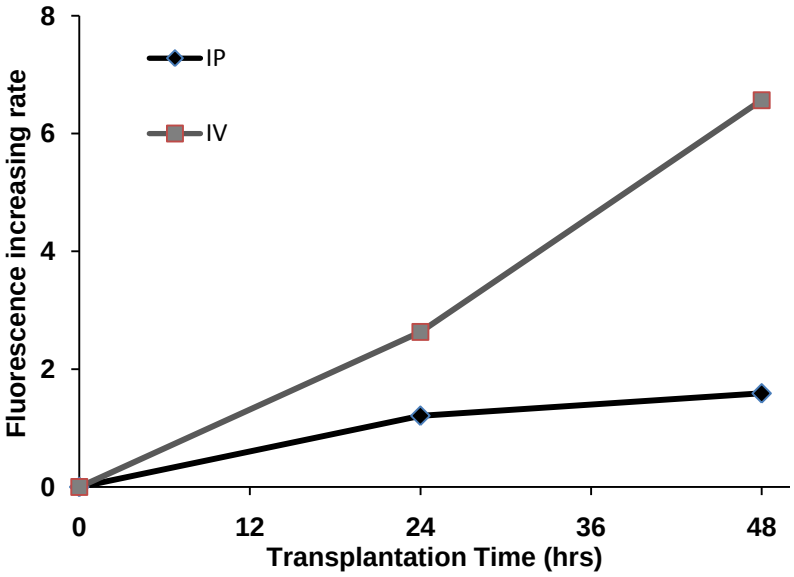

(c)

Figure 10 Examination the distribution of MSCs using whole-body imaging system. Time points examined between the implantation areas fluorescence intensity with IV (a) and IP (b) injection with 24h, 48h (from left to right).(C) The signal intensity of IP site with IP injection was decreasing through time points. ○: Implantation area.

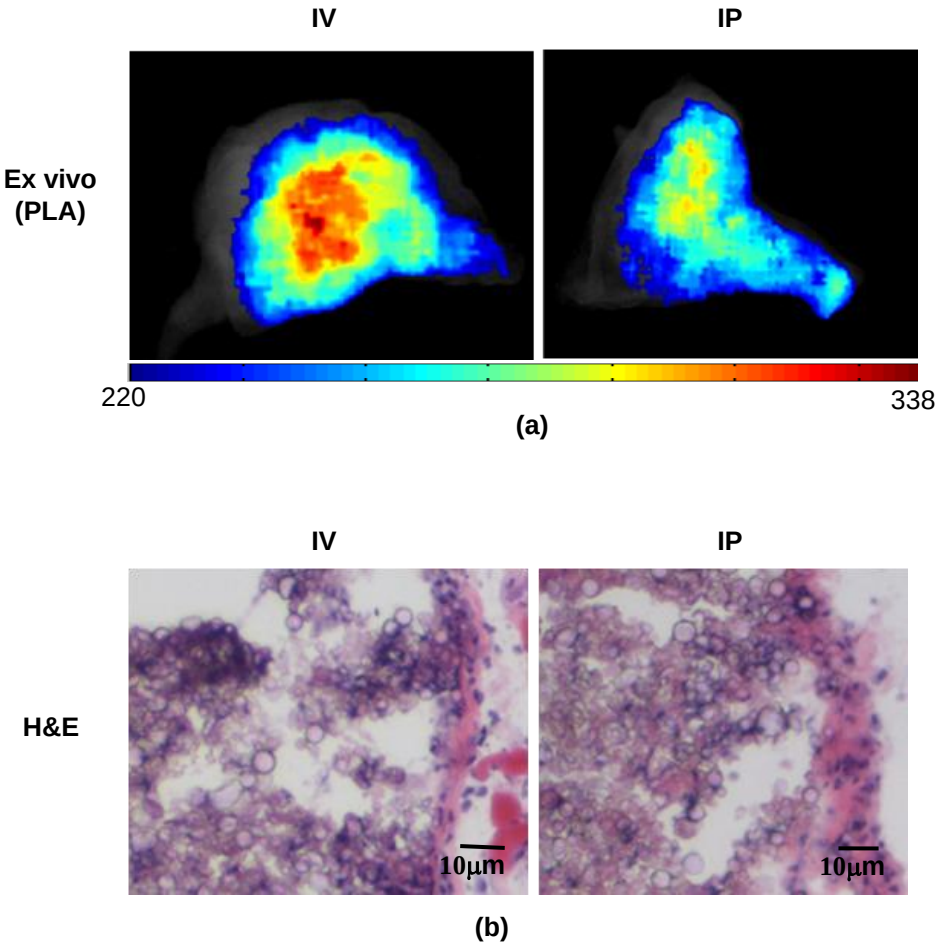

Figure 11 Histology results of PLA implants after 48hr examination. From left to right: IV injection, IP injection and another IP injection experiment. (a) Ex vivo results of PLA implant (b) H&E results of PLA implant.

At the end of the study (IP vs. IV transplantation), the PLA implant and its surrounding tissues were isolated and then frozen sectioned after 48hre implantation. The numbers of immigrated inflammatory cells were then quantified (Figure 11a). The correlation between *ex vivo* fluorescence intensity and histology cell counts was determined. We find that there is a very good relationship between the numbers of immune cells and the numbers of recruited MSCs surrounding PLA implants (Figure 11 b).

Overall our results have shown that subcutaneous cell transplantation model gave us the best relationship between cell numbers and fluorecence intensities. The IV injection shows lower capsule cell number around the implantation site compared to the IP injection in H&E result (Figure 11b). After quantification the relationship between ex vivo intensity and histology cell counted, the result indicated that IV showed higher signal intensity but lower cell density in implantation site and IP showed lower intensity but higher cell density (Figure 12).

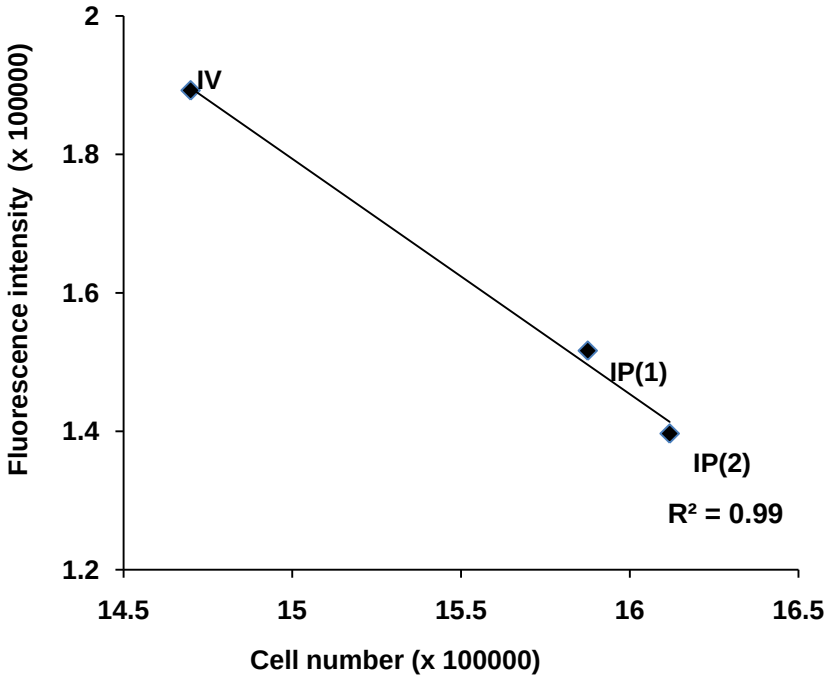

Figure 12 The correlation between implant fluorescence intensity and numbers of cells count in the capsule sites after 48hr examination.

MSCs migration toward the implantation site

Additional analyses were done to study the migration of MSCs from the peritoneal (ventral) transplantation sites to subcutaneous PLA implantation (dorsal) site. Immediately after IP transplantation, we saw large decrease of fluorescence intensity in the ventral part of mice indicating the emigration of MSCs out of the implantation sites (Figure 13a). The most reduction (~66%) of fluorescence intensity was found within the first 24 hours (Figure 13a). Between 24 and 48 hours, there is ~5% fluorescence reduction compared with initial fluorescence intensity. The

emigration of the MSCs is likely to be associated with the particle implants-mediated inflammatory responses, since the reduction of fluorescence in the ventral part of mice is much lesser in implant-free mice than in implant-bearing mice (Figure 13a). The reduction of fluorescence intensity in the ventral part of implant-free mice is in a relatively slow and constant rate compared with those of implant-bearing mice (Figure 13a).

Nearby the dorsal particle implantation site, we saw the fluorescence intensity dramatically increasing in implant-bearing mice compared to the implant-free mice (Figure 13b). The increasing of fluorescence intensity in the dorsal part of implant-free mice is in a relatively slow and constant rate compared with those of implant-bearing mice (Figure 13b).

3.4 Discussion

In this study, we investigated whether localized inflammatory responses could be triggered transplanted stem cells recruitment. To test the hypothesis, we used fluorescence imaging system and labeled cells with near-infrared dye (X-sight) to detach the stem cells migration in real-time. We detected a strong and specific fluorescence signal from the tissue around the PLA particle implant with different time points. The migration of the MSCs is likely to associate with particle implants-mediated inflammatory responses [29-32], since the reduction of fluorescence intensity in the ventral part of implant-free mice is in a constant slow rate compared with the implant-bearing mice. In support of our assumption, both CDFA-SE results counts and histological analysis also demonstrated the MSCs at the implantation sites of PLA particles over the course of the inflammatory response.

In addition to test MSCs recruitment, we used two different route for transplanted cells injection- Intravenous and intraperitoneal. Compared *in vivo* intensity after IV and IP injection of labeled MSCs, IV shows long time interval and higher signal intensity than IP after 48hr implantation. It is due to IP injection required resorption from peritoneal cavity to the blood stream [59], which reduced the circulation time, but might also reduced the labeled MSCs since IV injection directed injected into the blood stream. The quantification results indicated that the

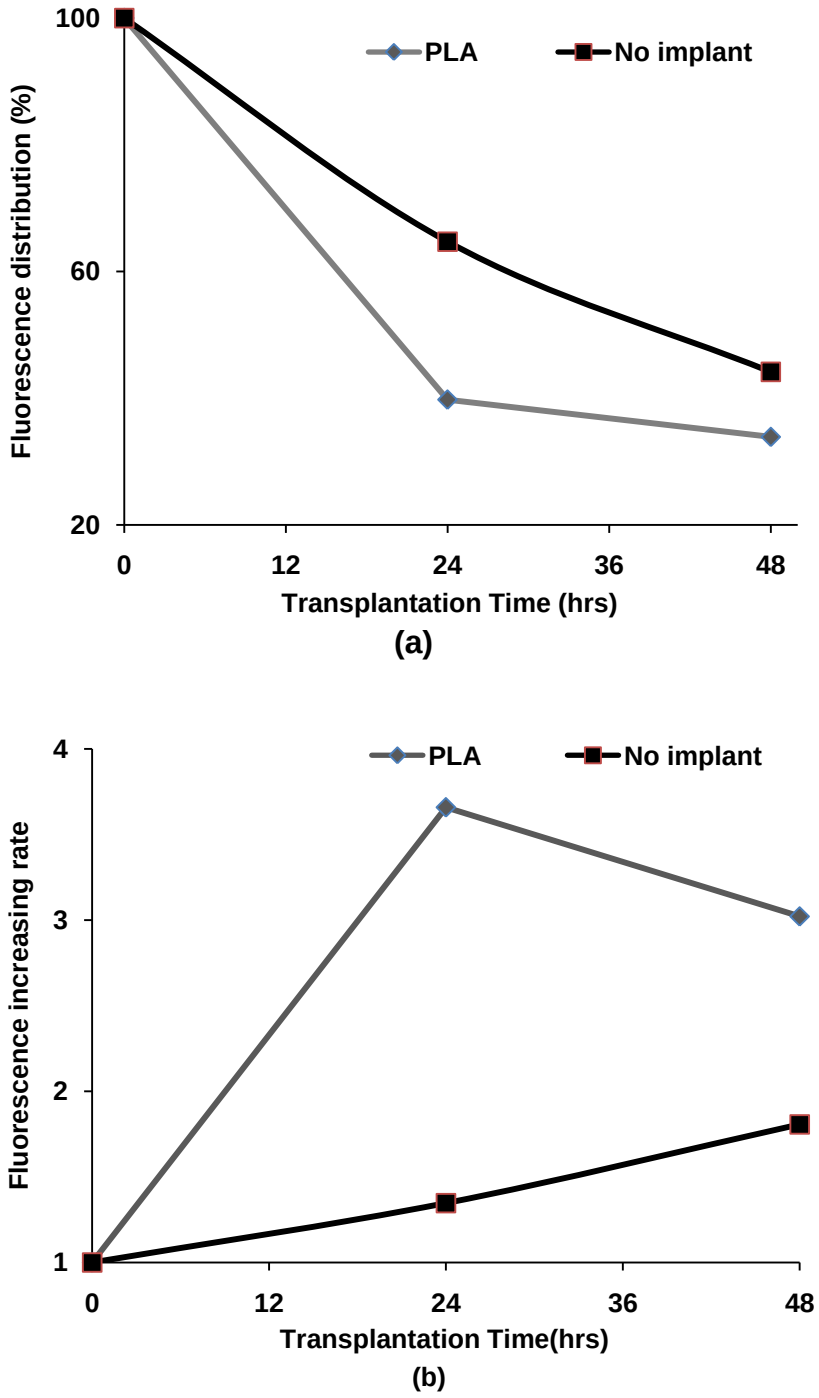

Figure 13 (a) Fluorescence intensity of the IP site with/without PLA implantation. The intensity of the peritoneal cavity decreasing through time point. (b) Fluorescence intensity of the implantation sites with/without PLA implantation. The intensity of the implantation sites increasing through time points.

correlation between signal intensity and cell density have a close relationship. Therefore, the implantation site of IV injection results in higher signal intensity and lower cell density. This relationship is reasonable due to when more stem cells recruitment to the inflammatory site it will undergo differentiation promoting structural and functional repair the injury sites [23, 42].

This imaging system can be able to detach the non-invasive high throughput the whole-body real-time fluorescence imaging to monitor the MSCs recruitment to localize inflammatory. Fluorescence imaging, relying upon the ability to detect and quantify the light originating from X-Sight labeled cells and animals, has been used to monitor the performance of stem cell combination implanted in living animals and the growth of cells on biomaterials [60, 61]. The ability to image the entire animal body with short acquisition time provides the benefit to monitor continually in the same animals.

CHAPTER 4

EFFECT OF LOCALIZED RELEASED CHEMOKINES ON STEM CELL ENGRAFTMENT IN TISSUE SCAFFOLDS (HYPOTHESIS II)

4.1 Rationale

Due to their plasticity and proliferative properties, stem cells have been used in numbers of tissue engineering study as the main sources of cells. Among all available sources of stem cells, autologous stem cells are undoubtedly the best sources of cells for fabricating tissue engineering products without potential ethic and biocompatibility concerns [18]. Unfortunately, autologous stem cells are not always accessible and often difficult to culture. In addition, MSCs seeded onto scaffolds often die following transplantation due to lack of oxygen and nutrients [18]. To date, new technology is needed to ensure the success of autologous stem cell tissue engineering.

It is well established that stem cells play an important role in wound healing reactions [24]. Several chemokines and cytokines have been indicated to involve in stem cells homing. Their function and the associated stem cell responses are listed below.

Stromal derived factor-1 alpha (SDF-1α) is a chemokine, critical to hematopoietic stem cell (HSC). SDF-1α has been found to be involved in inflammation models *in vivo* and considered as an important role in trafficking stem cells [20, 62]. This specific chemokine can regulate a variety of cellular functions, such as stem cell homing, trafficking, and differentiation. Stromal cell-derived factor-1α (SDF-1α) have been demonstrated to direct the migration of stem cells associated with injury repair in many species and tissue types [62].

Erythropoietin (EPO) is a glycoprotein hormone that controls red blood cell production. It is a cytokine for erythrocyte (red blood cell) precursors in the bone marrow, which also involved in the wound healing process. In the previous study that demonstrates the ability of EPO to stimulate hematopoietic stem cell proliferation [63]. As the major stromal cells in the bone

marrow, BM-MSCs have been known to release factors such as erythropoietin (EPO) supporting the survival, proliferation and differentiation of MSCs to enhance repair and regeneration of tissues [63]. EPO are cytokine known to enhance normal wound healing

Since stem cells have powerful regenerative properties and are widely used in tissue engineering to improve healing, our general hypothesis of this study is the following.

"In situ tissue engineering/regeneration can be achieved using scaffolds to release stem cell homing factors".

To test this hypothesis, it is critical to fabricate scaffolds which are capable of releasing a variety of cytokines and growth factors for a prolonged period of time (a few days to weeks). It should be noted that, despite of intensive research efforts, most of the scaffold fabrication technique cannot be used to load and to release proteins without complicated and expensive processes [20, 64]. Recently, our laboratory has developed microbubble scaffold fabrication techniques which can be used to load and to release a variety of proteins/chemokines/cytokines with a two-step process [65, 66]. This type of scaffold was used to test this hypothesis.

4.2 Methods and Materials

4.2.1 Materials

All the chemical and media were done as previous described (section 3.2.1).

4.2.2 Fabrication of chemokine releasing scaffolds

Gelatin scaffold were fabricated, and characterized as previous studies [20]. Briefly, the shell forming liquid consisted 10% gelatin (Sigma, St Louis, MO) mixed with either 1 µg/ml of SDF-1α (Prospec-Tany TechnoGene, Rehovot, Isreal) or 100 I.U. of EPO (Prospec-Tany TechnoGene, Rehovot, Isreal) in a glass test tube. Nitrogen gas was bubbles through the mixture while being sonicated using a probe sonicator (Ultrasonix, Bothell, WA) at 20 kHz for 10 seconds. The formation nitrogen gas was then filled microbubbles surrounded by a gelatin protein shell. Then the microbubbles were pipetted out and placed in glass tubes placed on a hot water bath with temperature maintain at 45^{o}C. The 75:25 poly (d, l-lactic-co-glycolic acid) PLGA was being

used in this experiment (Lakeshore Biomaterials, Birmingham, Al), 7.5%w/v PLGA was dissolved in 1, 4-dioxan (Aldrich, Milwaukee, WI) by vortexing on a Thermolyne type 16700 mixer for 30 minutes. The PLGA-dioxane mixture was poured into a Petri-dished and mixed with gelatin microbubbles. The polymer microbubble mixture was then lyophilized for 3 days. The porous gelatin scaffolds were cut into 3 x 3 x 3 mm cubes, and sterilized by soaking in 70% ethanol.

4.2.3 Bone marrow MSCs culture

Bone marrow derives MSCs culture was done as previous described (section 3.2.3).

4.2.4 Scaffold implantation and MSCs transplantation in mice

Cytokine release scaffolds were implanted subcutaneous on the lower back of Balb/c mice as described recently [20, 52]. In brief, after hair removal from the ventral surface and anesthesia then gelatin scaffolds with 10ul of 1ug/mL SDF-1 α or EPO contained (3x 3 x 1 mm) were implanted subcutaneous on one lower side of the back of Balb/C mice with control scaffold placed on the opposite site. For implantation, mice were anesthetized with isofluorane and the incision site marked and disinfected with 70% ethanol. After scaffold implantation for 24 hours, X-Sight labeling stem cells were injected on the IV or peritoneum (IP) area into the individual animals.

4.2.5 In vivo cell imaging

After MSCs transplantation for different periods of time (24 and 48 hours), the cell migration and distribution in vivo was then monitored using Kodak *In Vivo* Imaging system as described earlier (section 3.2.5).

4.2.6 Statistical analyses

Data analysis and statistical analyses were performed as described in section 3.2.7.

4.3 Results

4.3.1 Effects of microbubble scaffolds on stem cell recruitment in vivo

To examine whether microbubble scaffolds promote stem cell recruitment, the scaffolds were implanted on the lower back and then transplanted with labeled stem cell into the peritoneal cavity. As anticipated, we find that microbubble scaffolds triggered mild inflammatory responses (Figure 14, H&E stain). Furthermore, we have also observed that the fluorescence intensity at the IP cavity decrease through time, but increase at the microbubble scaffolds implanted area with time (Figure15&16, image and quantification). This shows that the microbubble scaffold prompted minimal stem cell recruitment.

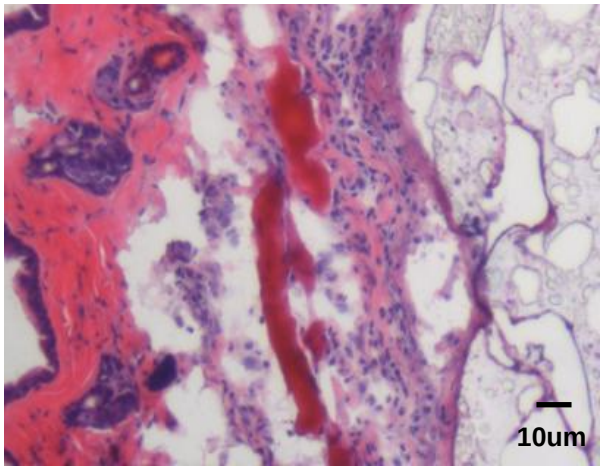

Figure 14 H&E results of microbubble scaffolds triggered mild inflammatory responses

4.3.2 Influence of chemokine released on intravenously transplanted stem cells

To study whether the localized release of stem cell homing factors on stem cell recruitment, SDF-1α-releasing and EPO-releasing gelatin scaffolds were fabricated and tested for their ability to recruit transplanted stem cells. Using the same animal model, chemokine releasing scaffolds were implanted on the back of mice. Twenty four hours later, X-sight-labeled MSCs were transplanted intravenously. After cell transplantation for 24 hours, the cell migration and distribution was then monitored in vivo. We find that, between 24 and 48 hours, there is

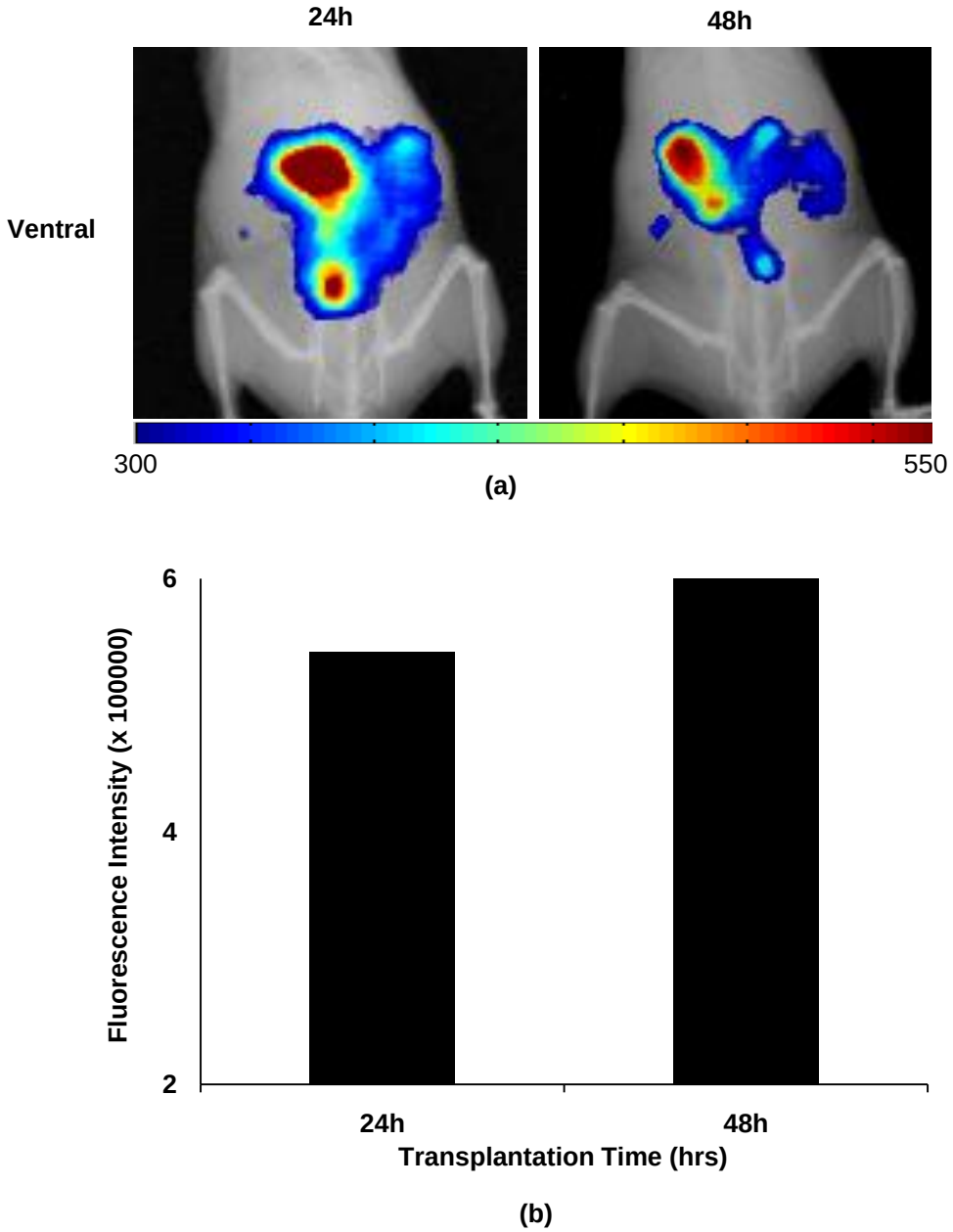

Figure 15 (a) Imaging results of microbubble scaffold result in 24hr and 48hr (left to right) at ventral position. (b) Different time points examined of peritonea cavity fluorescence intensity.

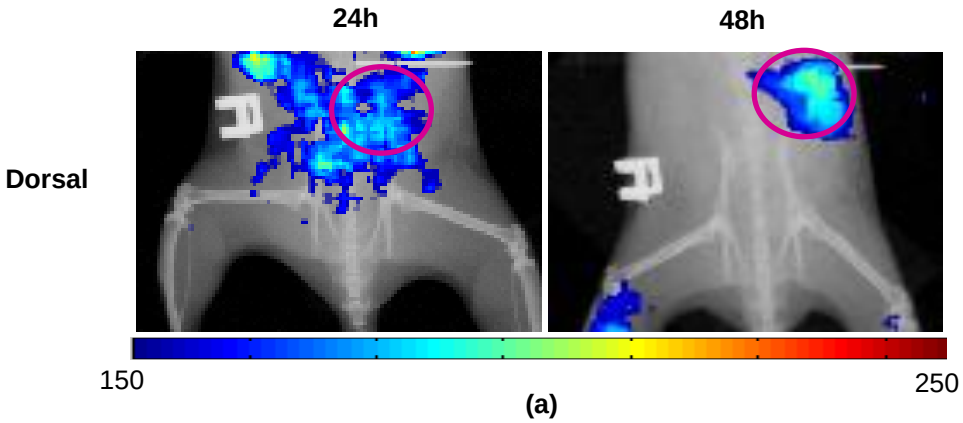

(a)

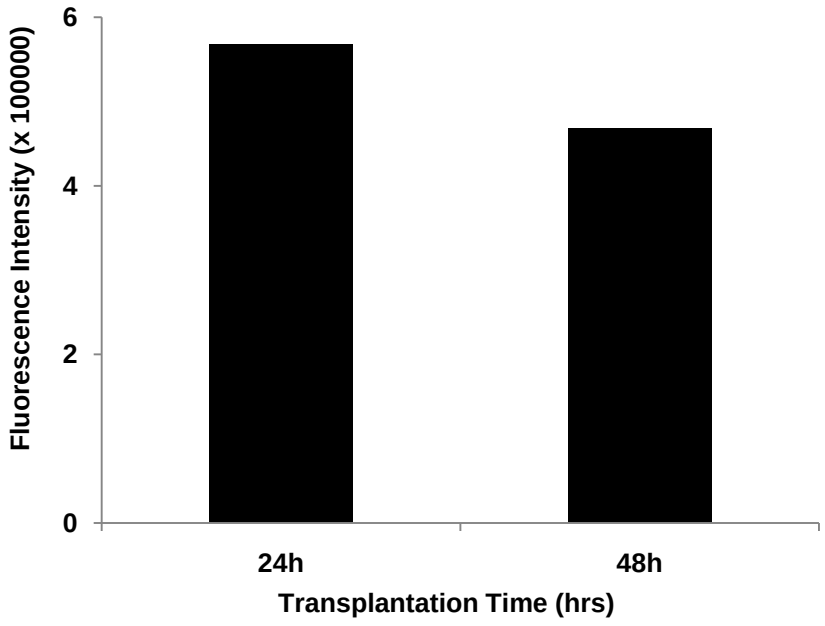

(b)

Figure 16 (a) Imaging results of microbubble scaffold implantation result in 24hr and 48hr (left to right) at dorsal position. (b) Different time points examined of implantation site fluorescence intensity. ○: Implantation area.

substantial recruitment of MSCs around the implantation sites (Figure 17a). Interestingly, we have also observed a very strong signal nearby the surgical incision site (Figure 17b). These results suggest that the injured tissue surrounding the incision site release powerful chemoattractant to recruit MSCs.

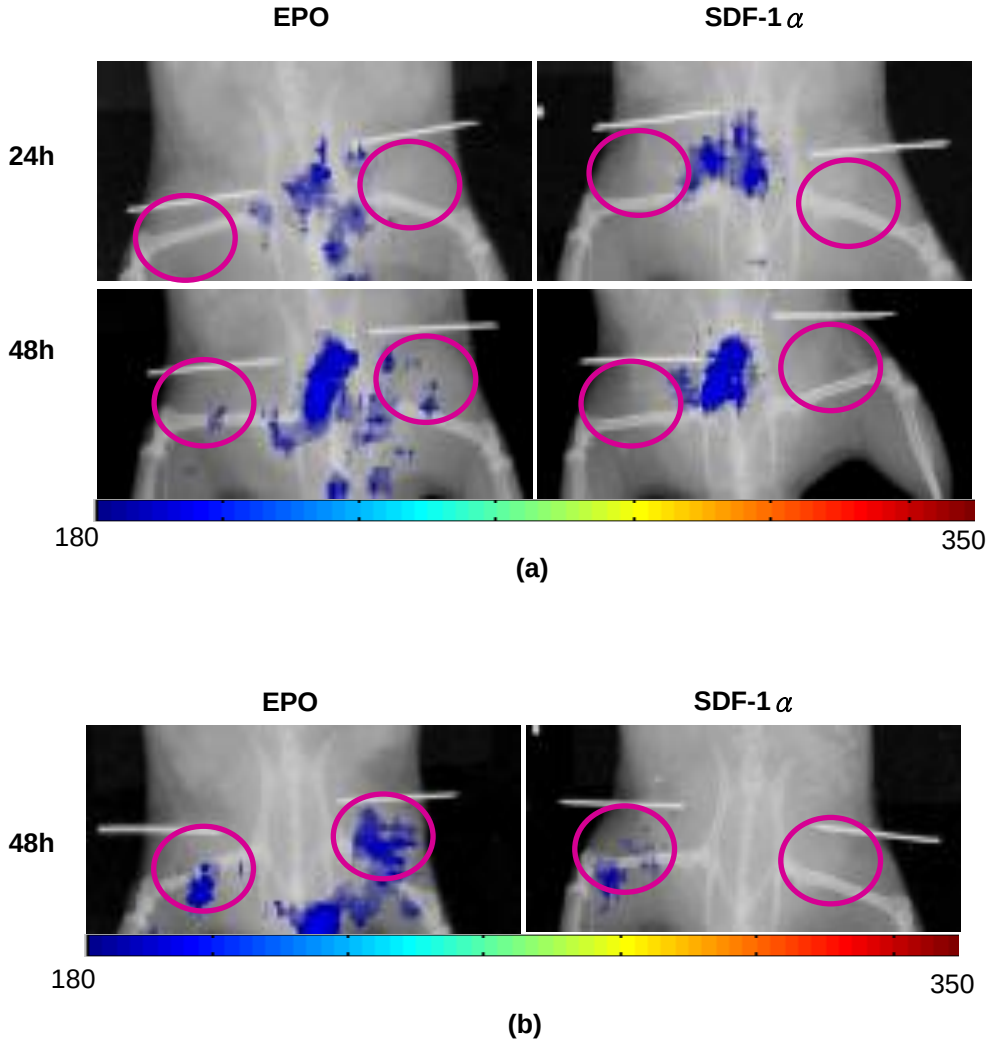

Figure 17 Homing of intravenously transplanted MSCs to subcutaneously implanted EPO-releasing and SDF-1-releasing scaffolds in mice. After MSCs transplantation for 48hr, the in vivo images of (a) L: EPO scaffold; R: SDF-1α scaffold (b) EPO scaffold and SDF-1α scaffold with blocking incision site, were taken. ○: Implantation area.

By comparing the cell responses to both types of scaffolds, we observed that the stem cells migration intensity on EPO loaded implant shows higher fluorescence intensity than SDF-1α loaded implant and control (Figure 18). Both the SDF-1α and EPO scaffolds at 24 hours and 48 hours resulted in significant increase in stem cell engraftment at the scaffold interface compared to the control scaffold (Figure 18). These results suggest that EPO might be a better choice for eliciting stem cell recruitment for in situ tissue engineering and regeneration.

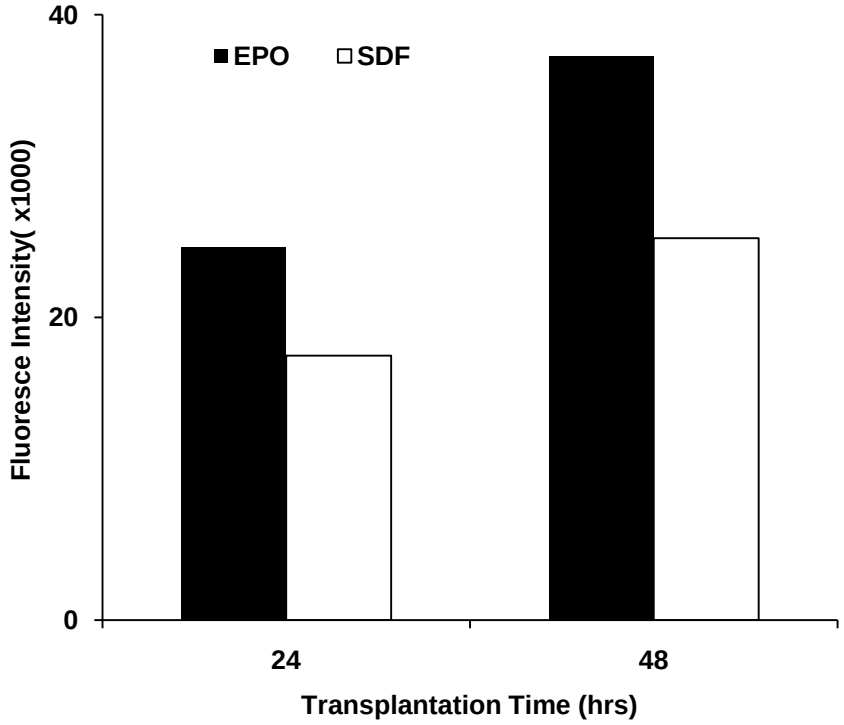

Figure 18 The extent of MSCs homing (reflected by fluorescence intensity) to either EPO-releasing or SDF-1α -releasing scaffolds in vivo.

4.3.3 Effect of chemokine release on intraperitoneally transplanted stem cells

Similar study was also carried out on intraperitoneally transplanted MSCs. We studied the effect of localized release chemokines on the recruitment of MSCs transplanted in the peritoneal cavity, instead of intravenous space. As expected EPO scaffolds were found to have attracted a substantially large number of stem cells compared to SDF-1α scaffolds (Figure 19a& b). Following cell transplantation for 48 hours injection, both EPO and SDF-1α scaffolds were still capable of engrafting and homing IP transplanted stem cells (Figure 19a&b).

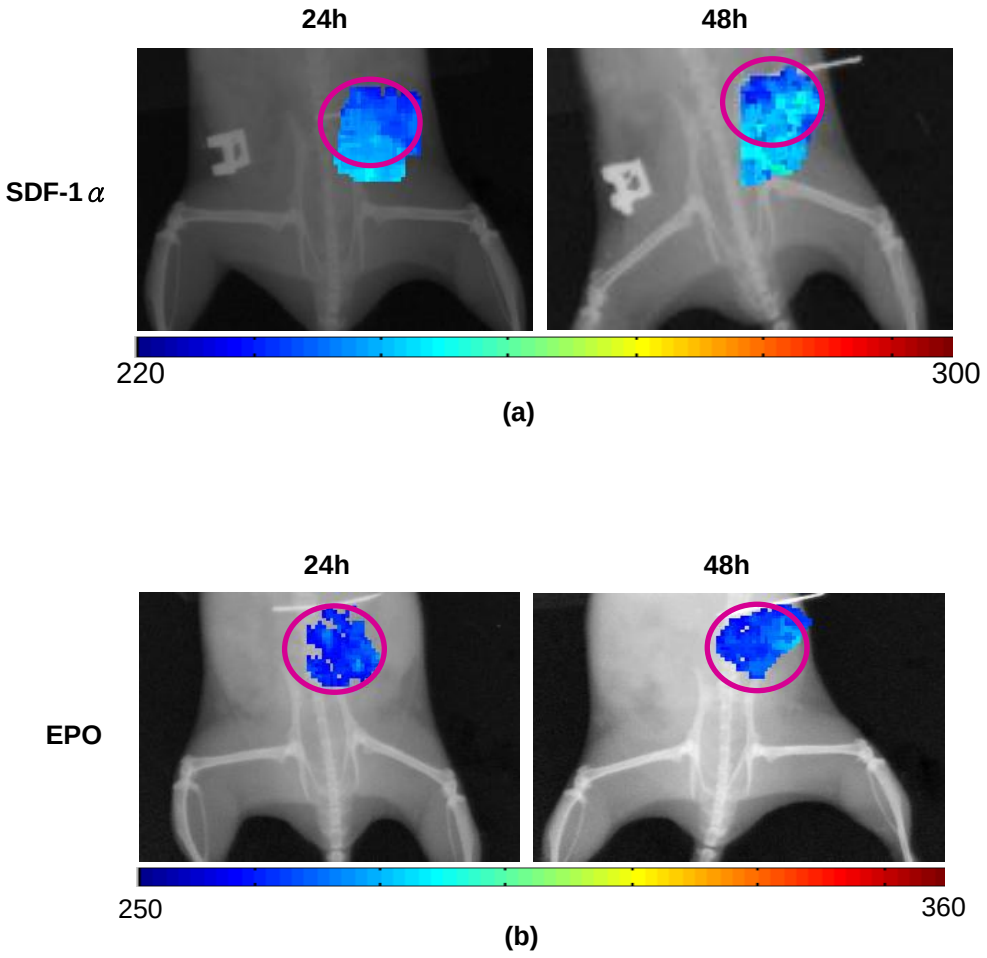

Figure 19 Homing of intraperitoneally transplanted MSCs to chemokine-releasing scaffolds in vivo. Images were taken at dorsal regions surrounding (A) EPO-releasing scaffold and (B) SDF-1α-releasing scaffold following MSCs transplantation for 24 and 48 hours (from left to right) ○: Implantation area.

Tissue sections were stained and the extent of tissue response was quantified based on the cell density at the interface (Figure 21). Our results showed that only a small number of MSCs were recruited to the control scaffolds. On the other hand, substantially stronger MSCs homing was found in the tissue surrounding either EPO- or SDF1α-releasing scaffolds (Figure 20a). By comparing both chemokines, EPO-releasing scaffolds trigger significantly more MSCs homing than SDF1α-releasing scaffolds (Figure 20a&b).

We have also examined the extent of inflammatory responses associated with variously treated scaffolds based on H&E staining. As expected, the control scaffold implants were characterized by the thickest encapsulating cell layer as part of the development inflammatory

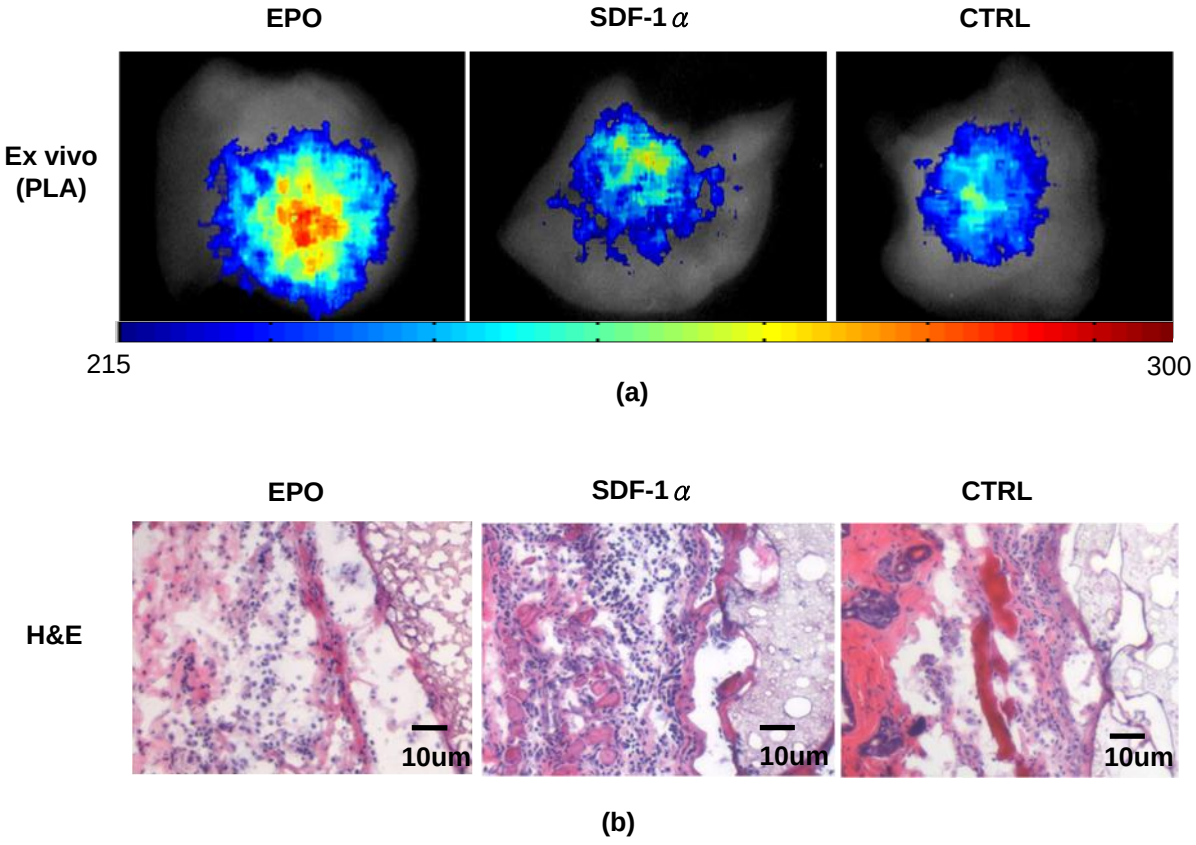

Figure 20 Effect of chemokine release on MSCs and immune reactions to scaffold implants in vivo. (a) MSCs homing can be quantified based on ex vivo images of scaffold implant. (b) The extent of tissue responses to implants was determined based on H&E staining. From left to right: EPO-releasing scaffold, SDF-1α-releasing scaffold, and control Scaffold.

reaction around the scaffold implants (Figure 21 a). Unexpectedly, we find that both EPO-releasing scaffolds and SDF-1α-releasing scaffolds resulted thinner capsule layers compare to the control (Figure 21a). In addition, cell numbers associated with SDF-1α-releasing scaffolds and EPO-releasing scaffolds were substantially less than control scaffolds (Figure 21b). Interestingly, there is a reverse relationship (R^2=0.85) between MSCs recruitment and inflammatory responses in vivo (Figure 22). This relationship suggested that the localized release of either SDF-1α or EPO resulted in significant increase in stem cell engraftment and reduction in inflammatory responses at the scaffold interface compared to the control scaffold (Figure 20).

4.4 Discussions

Our results lend strong support that this imaging system can be able to detach the non-invasive high throughput the whole-body real-time fluorescence imaging to monitor the MSCs recruitment to localize inflammatory. The results indicated that the migration of the MSCs is likely to associate with foreign implants-mediated inflammatory responses. Another fluorescent compound CFDA-SE was being used to evaluate the amount of MSCs migration [57, 58]. Overall our results have shown that subcutaneous cell transplantation model gave us the best relationship between cell numbers and fluorecence intensities. CFDA-labeled MSCs were difficult to be identified in tissue due to low cell numbers, but the relationship between CFDA-labeled MSCs numbers and fluorescence intensities has a reasonable correlation. Even though the correlation results in linear, the variations of all CFDA-labeled MSCs counting data are large.

In the absence of extrinsic stimulation, strong fluorescence intensity was detected in the peritoneal cavity for a prolonged period of time suggesting the weak emigration of transplanted MSCs. However, with distal inflammation (subcutaneous scaffold implants), we find that many of the IP transplanted MSCs migrated out of the intraperitoneal space in a short period of time. The decreasing percentage between PLA implant and implant-free mice is about ~70% (PLA implant)

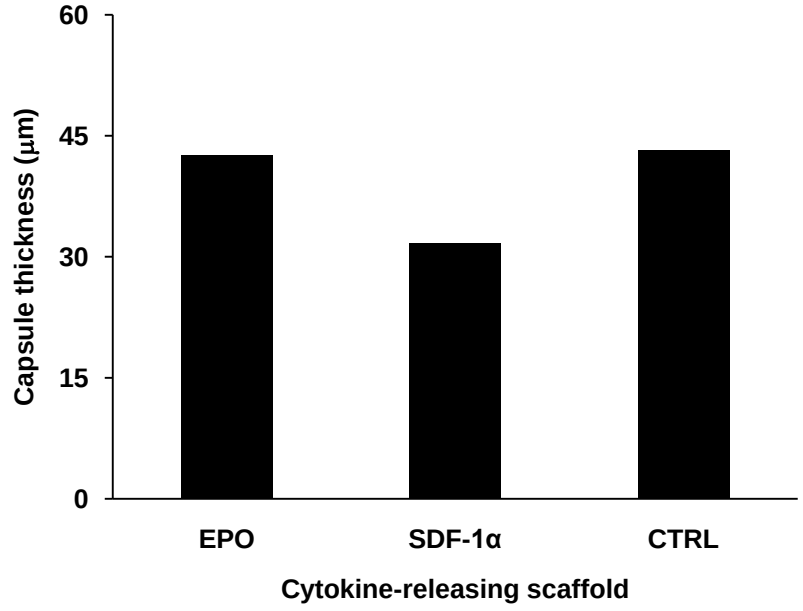

(a)

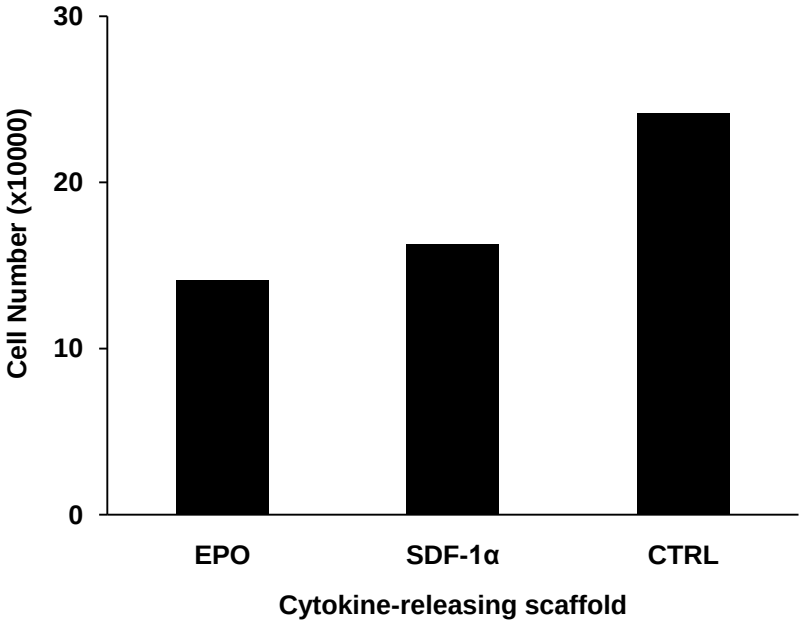

(b)

Figure 21 Histology results of scaffold implants after 48hr examination. (a) Capsule thickness (b) Capsule cell number density counts.

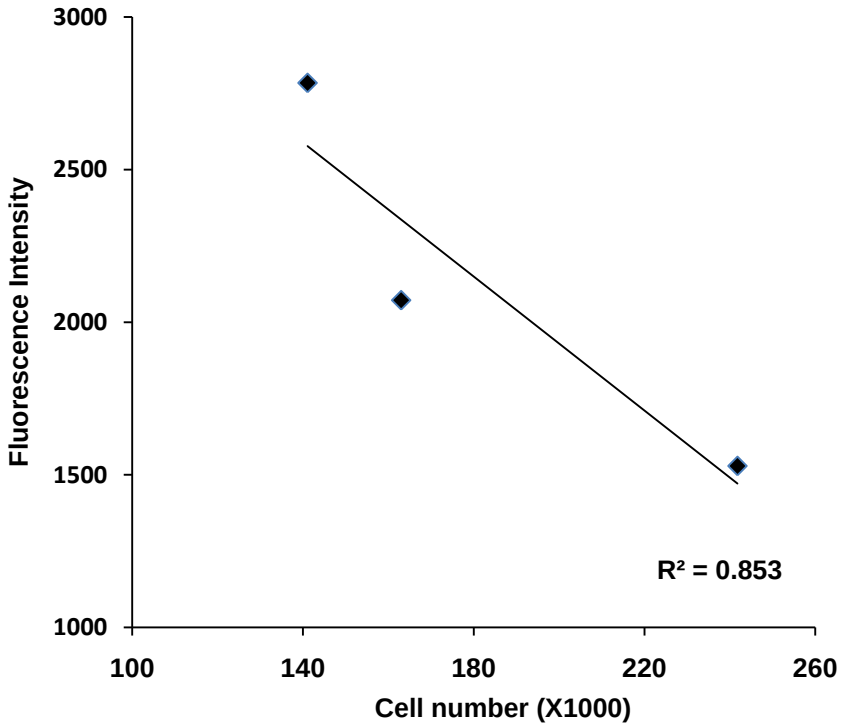

Figure 22 The correlation between implants intensity and capsule cell density counts was determined.

and ~50% (implant-free) at the peritoneal cavity, and the increasing 3 times and 1.8 times in the dorsal side. The quantification results indicated that the correlation between signal intensity and implant capsule cell density have a close relationship. This result indicated that with implantation, most of the transplanted MSCs were migrated to the inflammatory site, and the implant-free has less MSCs migrated.

Recently, it has shown that the inflammatory stimuli due to the scaffold implantation in combination with SDF-1α is likely to be the factor that leading to increasing beyond those stem cells recruited to participate in healing [52]. Compared both in vivo and ex-vivo examination of EPO and SDF-1α loaded scaffold implanted sites, EPO treated scaffolds shows higher signal intensity and thicker capsule length than SDF-1α after 48 hr implantation. These results suggest that EPO might be a better choice for producing stem cell recruitment scaffolds. When histology

examining of the inflammatory response to EPO, SDF-1α treated scaffolds and control scaffold, it is surprised to find that the control implanted scaffold resulted a thickest encapsulating cell layers than EPO and SDF-1α treated scaffold. In addition, comparison of the inflammatory cell density, both EPO and SDF-1α treated scaffold implants have lower cell density than control. Previously studies have provided the evidence that with localized released SDF-1α decreased inflammatory cell recruitment and enhance MSC migration [52, 67-70]. This indicated that the results of the localized release EPO and SDF-1α scaffolds can help increase the recruitment of stem cell populations to the site of scaffold implantation, but it also lead to significant decrease inflammatory cell accumulation and encapsulation of the scaffolds. An interesting finding that at the surgical incision sites of scaffold implant mice was observed strong signal intensity. This result also provides evidence that at the injured tissue surrounding the incision site release powerful chemoattractant to recruit MSC [24, 71].

The intraperitoneal transplanted cells migrate throughout the whole body via IP system therefore, the IP signal intensities decrease through the time. This specific circulation reduced the time of transplanted cells migration. The intensity at the scaffold implantation site provides an evidence of the labeled MSCs migration [59]. This result indicated that the intraperitoneal transplanted cells migrate throughout the IP system to the implantation sites; therefore, with the time change, the IP signal intensities decrease and the implant site intensities increase. The opposite results also observe in IV transplanted cell injection, the transplanted cells were directed injected into the blood stream. Therefore, the intensity of the peritoneal cavity increasing through time change, it take long time interval for MSC migrated to the implantation site through the blood stream, but results a stronger signal intensity. These findings suggest that recruitment of transplanted stem cells may be a viable approach to improve both the tissue response and regenerative potential of tissue engineering materials.

REFERENCES

1. Vats A, Tolley NS, Bishop AE, and Polak JM. Embryonic stem cells and tissue engineering: delivering stem cells to the clinic. *J. R. Soc. Med*. 2005; 98: 346–350.
2. Kim DE, Schellingerhout D, Ishii K, Shah K, and Weissleder R. Imaging of Stem Cell Recruitment to Ischemic Infarcts in a Murine Model. *Stroke.* 2004; 35:952-957.
3. Zhang SJ and Wu JC. Comparison of Imaging Techniques for Tracking Cardiac Stem Cell Therapy. *J. Nucl. Med..* 2007; 48: 1916-1919.
4. Gao X, Yang L, Petros JA, Marshall FF, Simons JW, and Nie S. I*n vivo* molecular and cellular imaging with quantum dots. *Biotechnol.* 2005; 16: 63-72.
5. Chapman AR, Frankel MS, and Garfinkel MS. Stem Cell Research and Applications Monitoring the Frontiers of Biomedical Research. *Ass'n for the advancement of sci., inst. For civ. Soc'y,* 1999.
6. Docherty K, Bernardo AS, and Vallier L. Embryonic stem cell therapy for diabetes mellitus. *Semin Cell Dev Bio*. 2007; 18: 827-838.
7. Koch CA, Geraldes P, and Platt JL. Immunosuppression by Embryonic Stem Cells. *Stem cells*. 2007; 26:89-98.
8. Takahashi K, Tanabe K, Ohnuki M, Narita M, Ichisaka T, Tomoda K, Yamanaka S. Induction of pluripotent stem cells from adult human fibroblasts by defined factors. *Cells*. 2007; 131:861–872.
9. Yu J, Vodyanik MA, Smuga-Otto K, Antosiewicz-Bourget J, Frane JL, Tian S, Nie J, Jonsdottir GA, Ruotti V, Stewart R, Slukvin II, and Thomson JA. Induced Pluripotent Stem Cell Lines Derived from Human Somatic Cells. *Science.* 2007; 318:1917-1920.
10. Stadtfeld M, Nagaya M, Utikal J, Weir G, and Hochedlinger K. Induced pluripotent stem cells generated without viral integration. *Science.* 2008; 322:945-949.

11. Fanò G, Tano GD, Parabita M, Beltramin A, and Mariggiò MA. Stem Cells in Adult Skeletal Muscle Tissue: More than a Working Hypothesis. *Basic Appl Myol.* 2004; 14:13-15.

12. Poulsom R, Forbes SJ, Hodivala-Dilke K, Ryan E, Wyles S, Navaratnarasah S, Jeffery R, Hunt T, Alison M, Cook T, Pusey C, and Wright NA. Bone marrow contributes to renal parenchymal turnover and regeneration. *J Pathol* .2001; 195:229–235.

13. Pittenger MF, Mackay AM, Beck SC, Jaiswal RK, Douglas R, Mosca JD, Moorman MA, Simonetti DW, Craig S, and Marshak DR. Multilineage Potential of Adult Human Mesenchymal Stem Cells. *Science*. 1999; 284: 143-147.

14. Guan G, Shi S, and Kramer PR. Role of Adult Stem Cells in Craniofacial Growth and Repair. *Semin Orthod.* 2005; 11: 227-233.

15. Koh CJ and Atala A. Tissue Engineering, Stem Cells, and Cloning: Opportunities for Regenerative Medicine. *J Am Soc Nephrol.* 2004; 15: 1113–1125.

16. Champlin R, and Ippoliti C. Supportive Care Manual for Blood and MarrowTransplantation. *Armonk, NY: Summit Communications*. 2007.

17. Hoffman R, Benz EJ, Shattil SJ, Furie *B and* Cohen HJ. Hematology*:* basic principles and practice*. Churchill Livingstone.*1991; 1409-1415.

18. Brenner M, Mirro J, Hurwitz C, Santana V, Ihle J, Krance R, Ribeiro R, Roberts WM, Mahmoud H, Schell M, Garth K, Moen RC, and French-Anderson WF. Autologous bone marrow transplant for children with AMC in first complete remission: use of marker genes to investigate the biology of marrow reconstitution and mechanism of relapse. *Hum Gene Ther*. 1991; 2: 137-159.

19. Melero-Martin JM, Khan ZA, Picard A, Wu X, Paruchuri S, and Bischoff J. In vivo vasculogenic potential of human blood-derived endothelial progenitor cells. *Blood*. 2007; 109 : 4761-4768.

20. Nair A. Novel preparation of polymeric scaffolds for tissue engineering using phase separation with protein microbubble incorporation. *Master's thesis,* University of Texas at Arlington, 2006.

21. Viola J, Lal B, and Oren G. The emergence of tissue engineering as a research fields. *Emerg Tissue Eng.* 2003; 5-7.

22. Polak JM and Bishop AE. Stem Cells and Tissue Engineering: Past, Present, and Future. *Ann YT Acad Sci.* 2006; 1068:352–366.

23. Diegelmann RF, Lindblad WJ, and Cohen IK. A subcutaneous implant for wound healing studies in humans. *J Surg Res.* 1986; 40:229-237.

24. Branski LK, Gauglitz GG, Herndon DN and Jeschke MG. A review of gene and stem cell therapy in cutaneous wound healing. *Burns*. 2009; 35: 171-180.

25. *Klein A, Talvani A, Cara* DC*, Gomes KL, Lukacs* NW, *and Teixeira MM.* Stem Cell Factor Plays a Major Role in the Recruitment of Eosinophils in Allergic Pleurisy in Mice Via the Production of Leukotriene B_4. *J Immunol*. 2000; 164: 4271-4276.

26. Boyle EM, Pohlman TH, Johnson MC, and Verrier ED. Endothelial Cell Injury in Cardiovascular Surgery: The Systemic Inflammatory Response. *Ann Thorac Surg* .1997; 63:277-284

27. DiPietro LA and Polverini PJ. Angiogenic macrophages produce the angiogenic inhibitor thrombospondin 1. *Am J Pathol*. 1993; 143: 678–684.

28. Oliveira SHP and Lukacs NW. Stem cell factor and IgE-stimulated murine mast cells produce chemokines (CCL2, CCL17, CCL22) and express chemokine receptors. *Inflamm. res*. 2001; 50:168–174

29. Abarbanell AM, Coffey AC, Fehrenbacher JW, Beckman DJ, Herrmann JL, Weil B, and Meldrum DR. Proinflammatory Cytokine Effects on Mesenchymal Stem Cell Therapy for the Ischemic Heart. *Annu Thor Surgery*. 2009; 88: 1036-1043.

30. Stroo I, Stokman G, Teske GJD, Florquin S and Leemans JC. Haematopoietic stem cell migration to the ischemic damaged kidney is not altered by manipulating the SDF-1/CXCR4-axis. *Nephrol Dial Transpl*. 2009; 24:2082-2088.

31. Read LR, Cumberbatch JA, Buhr MM, Bendall AJ and Sharif S. Cloning and characterization of chicken stromal cell derived factor-1. *Dev Com. Immunol.* 2005; 29:143-152.

32. Kollet O, Shivtiel S, Chen YQ, Suriawinata J, Thung SN, Dabeva MD, Kahn J, Spiegel A, Dar A, Samira S, Goichberg P, Kalinkovich A, Arenzana-Seisdedos F, Nagler A, Hardan I, Revel M, Shafritz DA, and Lapidot T. HGF, SDF-1**,** and MMP-9 are involved in stress-induced human CD34+ stem cell recruitment to the liver. *J Clin Invest.* 2003; 112:160–169.

33. Chen X, Oppenheim JJ and Howard OMZ. Chemokines and Chemokine Receptors as Novel Therapeutic Targets in Rheumatoid Arthritis (RA): Inhibitory Effects of Traditional Chinese Medicinal Components. *Cell Mol Immunol*. 2004; 1:336-342.

34. Chen L, Tredget EE, Wu PYG, and Wu Y. Paracrine Factors of Mesenchymal Stem Cells Recruit Macrophages and Endothelial Lineage Cells and Enhance Wound Healing. *PLoS ONE*. 2008; 3: e1886.

35. Heeschen C, Aicher A, Lehmann R, Fichtlscherer S, Vasa M, Urbich C, Mildner-Rihm C, Martin H, Zeiher AM, and Dimmeler S. Erythropoietin is a potent physiologic stimulus for endothelial progenitor cell mobilization. *Blood.* 2003; 102:1340-1346.

36. Arefieva TI, Kukhtina NB, Antonova OA, and Krasnikova TL. MCP-1-stimulated chemotaxis of monocytic and endothelial cells is dependent on activation of different signaling cascades. *Cytokine*. 2005; 31: 439-446.

37. Charo IF, and Ransohoff RM. The many roles of chemokines and chemokine receptors in inflammation. *N Engl J Med*. 2006; 354:610-621.

38. Castellani ML, Vecchiet J, Salini V, Conti P, Theoharides TC, Caraffa A, Antinolfi P, Teté S, Ciampoli C, Cuccurullo C, Cerulli G, Felaco M, and Boscolo P. Stimulation of CCL2 (MCP-1) and CCL2 mRNA by substance P in LAD2 human mast cells. *Transl Res.* 2009; 154:27-33.

39. Toh K, Kukita T, Wu Z, Kukita A, Sandra F, Tang QY, Nomiyama H, and Iijima T. Possible involvement of MIP-1alpha in the recruitment of osteoclast progenitors to the distal tibia in rats with adjuvant-induced arthritis. *Lab Invest.* 2004; 84:1092-102.

40. McLaughlin W and Vizard D. *In vivo* imaging system: precise coregistration of molecular imaging with anatomical X-ray imaging in animals. *Nat Med*. 2006:26-28.

41. Zinn KR, Chaudhuri TR, Szafran AA, Q'Quinn D, Weaver C, Dugger K, Lamar D, Kestersom RA, Wang X, and Frank SJ. Noninvasive bioluminescence imaging in small animals. *Ilar J.* 2008; 49: 103-115.

42. Okada S, Ishii K, Yamane J, Iwanami A, Ikegami T, Katoh H, Iwamoto Y, Nakamura M, Miyoshi H, Okano HJ, Contag CH, Toyama Y, and Okano H. In vivo imaging of engrafted neural stem cells: its application in evaluating the optimal timing of transplantation for spinal cord injury. *The FASEB Journal*. 2005: 1839-1841.

43. Saldanha KJ, Piper SL, Ainslie KM, Desai TA, Kim HT, and Majumdar S. Magnetic resonance imaging of iron oxide labeled stem cells: applications to tissue engineering based regeneration of the intervertebral disc. *Eur Cells Mater*. 2008; 16:17-25.

44. Weisslede R. Scaling down imaging: Molecular mapping of cancer in mice. *Nat Rev Cancer*.2002; 2:1-8.

45. Parak WJ, Pellegrino T and Plank C. Labelling of cells with quantum dots. *Nanotechnology.* 2005; 16: R9-R25.

46. Lawrence D. True, and Xiaohu Gao. Quantum Dots for Molecular Pathology. *J Mol Diagn*. 2007; 9: 7–11.

47. Medintz IL, Uyeda HT, Goldman ER, and Mattoussi H. Quantum dot bioconjugates for imaging, labeling and sensing. *Nat. Mater*. 2005; 4:435-446

48. Tang L and Eaton JW. Natural responses to unnatural materials: A molecular mechanism for foreign body reactions. *Mol Med*. 1999; 5: 351–358.

49. Tang L, Jennings TA, and Eaton JW. Mast cells mediate acute inflammatory responses to implanted biomaterials*. Proc. Natl. Acad.Sci.* 1998; 95: 8841-8846.

50. Widera D, Holtkamp W, Entschladen F, Niggemann B, Zänker K, Kaltschmidt B, and Kaltschmidt C. MCP-1 induce migration of adult neural stem cells. *Eur J Cell Bio.* 2004; 83: 381-387.

51. Tang J, Wang J, Yang J, Kong X, Zheng F, Guo L, Zhang L, and Huang Y. Mesenchymal stem cells over-expressing SDF-1 promote angiogenesis and improve heart function in experimental myocardial infarction in rats. *Eur J Cardio-Thorac.* 2009; 36: 644-650.

52. Thevenot P, Nair A, Shen J, Lotfi P, KO CY, and Tang L. The effect of incorporation of SDF-1 into PLGA scaffolds on stem cell recruitment and the inflammatory response. *Biomaterial.* 2010; 31: 3997-4008.

53. Zhang G, Nakamura Y, Wang X, Hu Q, Suggs LJ, and Zhang J. Controlled release of stromal cell-derived factor-1 alpha in situ increase c-kit+ cell homing to the infracted heart. *Tissue Eng.* 2007; 1: 2063-2071.

54. Graves EE, Weissleder R, Ntziachristos V. Fluorescence molecular imaging of small animal tumor models. *Curr Mol Med.* 2004; 4:419-30.

55. Bulte JW, Duncan ID, and Frank JA. In vivo magnetic resonance tracking of magnetically labeled cells after transplantation*. J Cereb Blood Flow Metab.* 2002; 22: 899-907.

56. Fiorina P, Jurewicz M, Augello A, Vergani A, Dada S, Rosa S, Martin Selig M, Godwin J, Law K, Placidi C, Smith RN, Capella C, Rodig S, Adra C, Atkinson M, Sayegh MH and Abdi R. Immunomodulatory Function of Bone Marrow-Derived Mesenchymal Stem Cells in Experimental Autoimmune Type 1 Diabetes. *J Immunol*. 2009; 183: 993 -1004.

57. Fuller ME, Mailloux BJ, Zhang P, Streger SH, Hall JA, Vainberg SN, Beavis AJ, Johnson WP, Onstott TC, and DeFlaun MF. Filed-scale evaluation of CFDA/SE staining coupled with multiple detection methods for assessing the transport of bacteria in situ. *FEMS Microbiol Ecol.* 2001; 37: 55-66.

58. De Clerck LS, Bridts CH, Mertens AM, Moens MM, and Stevens WJ. Use of fluorescent dyes in the determination of adherence of human leucocytes to endothelial cells and the effect of fluorochromes on cellular function. *J Immunol Methods* 1994; 172: 115-124.

59. Keyaerts M, Verschueren J, Bos TJ, Tchouate-Gainkam LO, Peleman C, Breckpot K, Vanhove C, Caveliers V, Bossuyt A, and Lahoutte T. Dynamic bioluminescence imaging for quantitative tumour burden assessment using IV or IP administration of D-luciferin: effect on intensity, time kinetics and repeatability of photon emission. *Eur J Nucl Mol Imaging*. 2008; 35: 999-1007.

60. Blum JS, Temenoff JS, Park H, Jansen JA, Mikos AG, Barry MA. Development and characterization of enhance green fluorescent protein and luciferase expressing cell line for non-destructive evaluation of tissue engineering constructs. *Biomaterials*. 2004; 25: 5809-5819.

61. Román I, Vilalta M, Rodriguez J, Matthies AM, Srouji S, Livne E, Hubbell JA, Rubio N ,and Blanco J. Analysis of progenitor cell-scaffold combinations by *in vivo* non-invasive photonic imaging. *Biomaterials.* 2007; 28: 2718-2728.

62. Schober A, Karshovska E, Zernecke A and Weber C. SDF-1α-Mediated Tissue Repair by Stem Cells: A Promising Tool in Cardiovascular Medicine? *Trends Cardiovas Med*. 2006; 16: 103-108.

63. Heeschen C, Aicher A, Lehmann R, Fichtlscherer S, Vasa M, Urbich C, Mildner-Rihm C, Martin H, Zeiher AM, and Dimmeler S. Erythropoietin is a potent physiologic stimulus for endothelial progenitor cell mobilization. *Blood.* 2003; 102: 1340-1346.

64. Thevenot P, Nair A, Dey J, Yang J, Tang L. Method to analyze three-dimensional cell distribution and infiltration in degradable scaffolds. *Tissue Eng Part C Methods.* 2008; 14: 319-331.

65. Nair A, Thevenot P, Dey J, Shen J, Sun MW, Yang J, Tang L. Novel polymeric scaffolds using protein microbubbles as porogen and growth factor carriers. *Tissue Eng Part C Methods.* 2010; 16: 23-32.

66. Kremer KN, Humphreys TD, Kumar A, Qian NX, and Hedin KE. Distinct Role of ZAP-70 and Src Homology 2 Domain-Containing Leukocyte Protein of 76 kDa in the Prolonged Activation of Extracellular Signal-Regulated Protein Kinase by the Stromal Cell-Derived Factor 1_/CXCL12 Chemokine. *J Immunol.* 2003; 171: 360-367

67. Yanshuang Xie, Kai Gao, Lari Häkkinen, Hannu S. Larjava. Mice lacking β6 integrin in skin show accelerated wound repair in dexamethasone impaired wound healing model. *Wound Repair Regen.* 2009; 17:326-339.

68. Jin DK, Shido K, Kopp HG, Petit I, Shmelkov SV, Young LM, Hooper AT, Amano H, Avecilla ST, Heissig B, Hattori K, Zhang F, Hicklin DJ, Wu Y, Zhu Z, Dunn A, Salari H, Werb Z, Hackett NR, Crystal RG, Lyden D, and Rafii S. Cytokine mediated deployment of SDF-1 induces revascularization through recruitment of CXCR4+ hemangiocytes. *Nat Med*. 2006; 12:557-567.

69. Stellos K, Langer H, Daub K, Schoenberger T, Gauss A, Geisler T, et al. Plateletderived stromal cell-derived factor-1 regulates adhesion and promotes differentiation of human CD34+ cells to endothelial progenitor cells. *Circulation*. 2008; 117:206-215.

70. Chen L, Tredget EE, Wu PY, Wu Y. Paracrine factors of mesenchymal stem cells recruit macrophages and endothelial lineage cells and enhance wound healing. *PLoS ONE* .2008; 3: 1886.

71. Imitola J, Raddassi K, Park KI, Mueller FJ, Nieto M, Teng YD, Frenkel D, Li J, Sidman RL, Walsh CA, Snyder EY, and Khoury SJ. Directed migration of neural stem cells to sites of

CNS injury by the stromal cell-derived factor 1α/CXC chemokine receptor 4 pathway. *Proc Natl Acad Sci U S A*. 2004; 101: 18117–18122.

BIOGRAPHICAL INFORMATION

Manwu Sun received her Bachelor of General Biology from the University of Texas at Arlington in Spring 2007. Manwu was born in Taiwan on October 27, 1983 and did her schooling and undergraduation there. She was accepted into the Biomedical Engineering program at the University of Texas at Arlington in Spring 2008, and left for the United States of America to pursue what was closest to her heart.

Manwu believes that tissue engineering is the future of medicine. She envisions a world where there are affordable tissue engineered solutions to the ailments plaguing mankind today, and this vision motivates her every single day to work tirelessly towards that ultimate goal.